

NASA TECHNICAL
REPORT



NASA TR R-280

2.1

NASA TR R-280

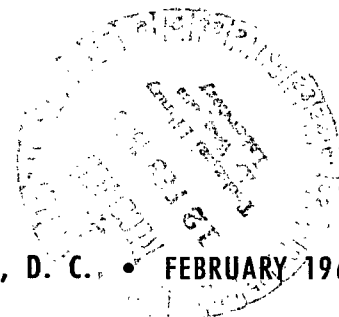


LOAN COPY: RETURN
AFWL (WLIL-2)
KIRTLAND AFB, N MEX

SIMULTANEOUS CORRECTION
OF VELOCITY AND MASS BIAS
IN PHOTOGRAPHY OF METEORS

by C. D. Miller
Lewis Research Center
Cleveland, Ohio

NATIONAL AERONAUTICS AND SPACE ADMINISTRATION • WASHINGTON, D. C. • FEBRUARY 1968





SIMULTANEOUS CORRECTION OF VELOCITY AND MASS
BIAS IN PHOTOGRAPHY OF METEORS

By C. D. Miller

Lewis Research Center
Cleveland, Ohio

NATIONAL AERONAUTICS AND SPACE ADMINISTRATION

For sale by the Clearinghouse for Federal Scientific and Technical Information
Springfield, Virginia 22151 - CFSTI price \$3.00

SIMULTANEOUS CORRECTION OF VELOCITY AND MASS

BIAS IN PHOTOGRAPHY OF METEORS

by C. D. Miller

Lewis Research Center

SUMMARY

In any statistical study of characteristics of meteors with data obtained from photographs, corrections must be made for two inherent biasing effects due to the brighter trails left by meteors of greater mass and/or by meteors of greater velocity relative to Earth's atmosphere. In the past, attempts have been made to correct for both biasing effects with a weighting factor inversely proportional to the square of the meteor velocity relative to atmosphere.

A new analysis has been made to investigate the magnitude of the weighting factor, specifically for application to photographic meteor data published by Smithsonian Institution Astrophysical Observatory. As a result of this analysis, a revised factor was obtained to operate upon actual counts of photographic meteors within various classes of velocity to provide a correct ratio of counts for all velocities reduced to any given lower mass limit.

In the analysis, an expression was derived theoretically for maximum effective exposure on the photographic plate produced by a meteor in terms of the original mass of the particle, its velocity relative to Earth's atmosphere, and the angle of its path to the zenith. The expression for maximum effective exposure was tested and revised by application to 100 test meteors that were believed to have provided approximately uniform effective exposure density. The revised expression for maximum effective exposure was combined with a widely accepted equation for the influx rate of meteors of mass greater than a stated value to obtain approximately the desired weighting factor. The manner of the combination eliminated mass of the meteor particle from the factor.

The analysis indicated a large change in value of the exponent of velocity relative to Earth's atmosphere in the weighting factor, namely, from -2 downward at least to -3.85 and possibly as low as -4.22 . Application of the new factor should cause a significant reduction of estimates of average meteor velocities relative to the atmosphere. Extensive changes would also be required in estimates of other parameters that might bear a systematic relation to meteor velocities.

INTRODUCTION

In long-term planning for future space missions, it is anticipated that powerplants of substantial capacity may be required on board a space vehicle. The only means for the rejection of waste heat from such powerplants will be radiation to space. Radiation of heat to space is inefficient in comparison with conduction and convection, which are freely utilized in the dissipation of waste heat in ground-based powerplants. For such reasons, the radiators of space powerplants are likely to be large, and hence they will present a considerable vulnerable surface to destructive impact by meteoroids, that is, by small particles floating or moving at high velocities through space. Meteoroids also represent a hazard to other spacecraft structures and components.

In order that the extent of the hazard may be estimated, it is necessary to have extensive and accurate knowledge about the concentration of such particles in space, their physical characteristics, and the nature of their movements. Of special importance relative to impact damage by a particular particle are the mass of the particle and its velocity relative to the impacted surface. For these reasons, an analysis was undertaken at the NASA Lewis Research Center to determine corrected mass and velocity distributions for impact of meteor particles upon the Earth's atmosphere.

In the photography of meteors, it is well known that particles striking the atmosphere at higher relative velocities are more likely to leave visible trails on the photographic emulsion. Also, particles of greater mass are more likely to be detected for the same reason. The result is that a count of meteors that occur within a given area of the sky and within a given time interval is substantially biased in favor of fast moving particles and heavy particles. Thus, a basic prerequisite for the planned analysis was an adjusting factor, or factors, by which the mass and velocity bias could be compensated.

The availability of such an adjusting factor, in fact, is crucial to most statistical studies involving photographic meteors, if even an approximation of actual rather than apparent distributions is sought. Such statistical studies must involve comparisons of the numbers of meteors in various categories involving functions of the mass, velocity, and other characteristics of the particles, including the various parameters of their orbits. Two such categories would, in general, involve different average velocities relative to the atmosphere if not different masses. Hence, effort is justified to assure the availability of a sound factor, or factors, for correction of the mass and the velocity bias.

Previous work on this subject, incidental to other objectives, resulted in two adjusting factors as presented by Whipple in reference 1. For meteors of velocity relative to the atmosphere greater than 19 kilometers per second, his correction factor was $\phi = v_{\infty}^{-2}$. Here v_{∞} represents velocity of the particle relative to the atmosphere before any deceleration has been caused by the atmosphere. For slower particles, his factor

was $\phi = 3v_{\infty}^{-2}$. Such adjusting factors were designed for use as multipliers that would operate on actual counts of meteors at various particle velocities to provide corrected relative counts, that is, the correct ratios of counts for different velocities. For velocities less than 19 kilometers per second, Whipple increased the adjusting factor threefold because of what he referred to as peculiarly long trails at these lower velocities.

In reference 2, published in 1961, McCrosky and Posen used the adjusting factor $\phi = v_{\infty}^{-2}$ for all velocities because the meteors of low velocity did not show the exceptional lengths that appeared to be characteristic in the earlier and much smaller sample considered by Whipple in reference 1. They commented that uncertainties in the velocity-mass law and in the number-luminosity law are such that attempted corrections for these effects would probably be in error by at least 1 in the velocity exponent.

In the Whipple derivation of adjusting factors, use was made of the Watson assumption (ref. 3) that, within any velocity interval, the number of meteoroids of mass greater than a given mass varies inversely as the given mass. Such assumption at that time appeared to represent the most likely condition. Since then, however, this assumption has been superseded generally by the opinion that the number of meteoroids of mass greater than a given mass varies inversely as a power of the given mass greater than one. A widely accepted value of this power is 1.34 (ref. 4). The changed exponent in the relation of lower mass limit to flux of meteoroids appeared to call for revision of the correction factor. Also, it appeared likely that some refinement might be made in the treatment of the effects of altitude in apparent brightness of a meteor and effective area of field of view of the camera, which are mutually compensating only in part.

Hawkins and Upton (ref. 4) presented a weighting factor as a function of excess of photographic magnitude above the plate threshold level. This weighting factor, however, does not meet the needs involved in the present study completely because it is tabular rather than analytic and because, in its dependence upon photographic magnitude, it involves both meteoroid mass and meteoroid velocity. Elimination of either velocity or mass from the weighting factor is desirable to allow independent study of the distributions of these two important variables.

For these reasons, a decision was made to attempt a new derivation of an adjusting factor. The theoretical derivation of a new adjusting factor that resulted from this attempt, together with an indicated degree of confirmation and empirical modification based on analysis of meteor data from reference 2, is presented herein.

METHOD OF PROCEDURE

In the development of an adjusting factor for the correction of velocity and mass

bias in the photography of meteors, quantitative determination is necessary for the parametric relations that control whether a meteor trail will be exposed on photographic plates sufficiently that it may be detected in later examination of the plates.

When a meteoroid encounters the upper atmosphere of the Earth, collision with air molecules causes a progressive gaseous erosion of the mass of the meteoroid, known as ablation. Progressive loss of kinetic energy also occurs, mostly within the ablated mass. Emission of light results, and a visible trail consequently may be exposed on photographic plates according to the actinic energy of the light emitted, the speed of the meteoroid, its direction of motion, and the distance of the meteoroid from the camera.

As the meteoroid descends to lower altitudes, the rate of ablation and consequent intensity of emission of light tends both to increase because progressively more dense air is encountered and to decrease because of decreasing mass and consequently decreasing frontal area of the meteoroid. At the same time, for a given intensity of light emission, exposure on the photographic plate usually increases because the meteoroid is approaching the camera ever more closely.

All effects described are strongly affected by the angle at which the meteoroid approaches the Earth's surface. At a larger angle of meteoroid path to the zenith, the meteoroid may be ablated more slowly, with less intense emission of light; yet it may lose a greater amount of mass at a given distance from the camera with consequent decreased exposure. Distance from camera is also affected by location of the meteor relative to the camera within the horizontal plane.

For the reasons discussed, photographic exposure is interrelated in a complex manner with meteoroid mass, meteoroid velocity, angle of path to the zenith, altitude above Earth's surface, and position of meteoroid relative to camera. According to the interrelation of these parameters, various meteors will produce their greatest photographic exposures at various altitudes. The problem is complicated even further by a phenomenon known as reciprocity failure, which causes photographic exposure to vary in efficiency with exposure duration.

The most dense level of effective exposure for a given meteor at any point in its path determines whether the photographic trail may be detected. Hence, it is necessary to derive the interrelation of the various parameters that determines the altitude at which the most dense effective exposure occurs, and in turn to determine the actual effective density of the exposure at that altitude. The theoretical derivation of such interrelation of parameters and a moderate degree of empirical revision of the analytic result constitute the first of three logical stages in the development of the desired adjusting factor for the correction of velocity and mass bias.

At the end of the first stage as described, the parametric interrelation is merely a criterion for the possibility of discovering a meteor trail. This interrelation is in no sense a correction factor by which actual counts of meteors within given velocity ranges

or different mass ranges may be multiplied to yield true relative counts. A rational correction factor, however, can be deduced from the discovery criterion derived in the first stage of the work in conjunction with a widely accepted relation between mass and influx rate of meteors. Such relation (ref. 4) may be expressed as

$$F_{>m} = \alpha m^{-\beta} \tag{1}$$

where $F_{>m}$ signifies influx rate of meteoroids, or frequency of encounter per unit exposed area of particles with mass greater than m , and α and β are constants. As mentioned earlier, a value of 1.34 is often used for β . (Most symbols are also defined in appendix A.)

The correction factor to be deduced will be a function only of the initial velocity of the meteoroid relative to Earth's atmosphere and the angle of its path to the zenith. The correction factor is proportional to the reciprocal of the probability that any meteor of mass greater than some value m , with a particular velocity and with a particular angle of its path to the zenith, will produce an exposure density greater than indicated by the discovery criterion. Hence, for all combinations of velocity and zenith angle, values of the correction factor may be computed. The actual counts of meteors falling within the various combinations of velocity and zenith angle may then be multiplied by the factors so computed, and the results will indicate corrected relative frequencies of encounter of meteoroids within the various combinations of velocity and zenith angle and referred to the same lower limit of mass. That is, the values of the correction factor will permit use of the following equation:

$$\frac{F_{>m(i)}}{F_{>m(j)}} = \frac{\varphi_{w(i)} F_{i0}}{\varphi_{w(j)} F_{j0}} \tag{2}$$

In equation (2), $F_{>m(n)}$ signifies the corrected frequency of encounter per unit area of particles of mass greater than m for a classification n of particles within a particular small range of velocity and within a particular small range of angle of path to the zenith. The symbol $\varphi_{w(n)}$ represents the correction factor for classification n . The symbol F_{n0} represents the observed frequency of encounter of particles of all masses and within classification n as determined by the discovery of photographed trails. The correction factor φ_w , free of any function of meteoroid mass, is of substantial analytical value because it permits statistical separation of the important variables, meteoroid velocity relative to the atmosphere and meteoroid mass.

The deduction of such a correction factor constitutes the second and third stages of the work. In the second stage, the effect of altitude on area of field of view of the

camera must be ignored. In the third stage, however, an approximate and tentative adjustment will be made upon the correction factor to account for greater probability of encounter of higher-altitude meteors due to larger area of the camera field of view. Confirmation of the value of such adjustment must depend upon later work.

THEORETICAL DEVELOPMENT OF RELATION FOR MARGINAL PHOTOGRAPHIC DENSITY

Basic equations are available in accordance with generally accepted theory that interrelate the mass of a meteor particle, its velocity relative to the atmosphere, air density, luminous intensity, ablation rate, and luminous efficiency. Good accounts of such theory, including extensive references to pertinent literature, are presented in references 5 to 9. The basic equations previously derived and published will be used without account of their derivations here.

Expression for Photographic Exposure

A logical first step in the theoretical effort of stage 1 as described earlier will be to obtain an expression for the true exposure on a photographic emulsion resulting from a meteor of a particular luminous intensity, at a particular altitude, and with a particular meteoroid velocity. Photographic exposure is defined as the product of exposure duration and image brightness on a photographic emulsion. That is,

$$E = I_i T \quad (3)$$

where E is exposure, I_i is image brightness, and T is the effective duration of exposure of the image on the part of the photographic emulsion in question. For a moving point source of light or a moving source of given dimensions, the duration of exposure is inversely proportional to image velocity. Hence, from equation (3),

$$E \propto I_i v_i^{-1} \quad (4)$$

where v_i is instantaneous velocity of the image.

The image brightness is directly proportional to the luminous intensity of the meteor, that is, the total luminous flux emanating from it, and inversely proportional to the square of the distance of the meteor from the camera. The distance of the meteor from the camera is a function of the meteor height above camera level and the position of the meteor within the camera field of view or, conversely, the location of the camera

relative to the position directly under the meteor on the surface of the Earth. Obviously, if the total field of view of a camera were negligibly small and if the line of sight of the camera were directed toward a particular part of the sky, then the distance from meteor to camera would be proportional to the altitude of the meteor above the camera level. For the real condition, involving a large field of view and an unspecified position of a meteor within that field, the distance of meteor from camera is in general greater for greater height of meteor above ground level, and perhaps may be approximately proportional to that height. At this stage, to avoid unnecessary complications involving positions of meteors within the field of view, the distance from meteor to camera is treated as directly proportional to the meteor height above ground level h_g and to a function of position of meteor within the field of view F_h , to be discussed later. Accordingly,

$$I_i \propto I_m h_g^{-2} F_h^{-2} \quad (5)$$

where I_m is luminous intensity of the meteor. At present, F_h may be regarded as a correction factor which is always given whatever arbitrary value may be needed, as between one meteor and another, in order to make proportionality (5) correct.

The image velocity v_i is proportional to the component of meteor velocity normal to the line interconnecting meteor and camera and inversely proportional to distance between the two. Neither of these two parameters can be determined without knowledge of field position. However, for the present purpose, image velocity may be expressed in a less definite manner as a function of velocity of the meteor, zenith angle Z_R , or angle between the zenith and the path of the meteor through Earth's atmosphere, the azimuth of the meteor path, the location of the meteor within the camera field of view, and the height of the meteor above ground level. It is well known that a camera operating at a great distance from the photographic object measures angular displacements and, hence, angular velocities. Thus, other things being equal, image velocity is proportional to meteor velocity and inversely proportional to distance of a meteor from the camera. At this stage, to the extent that image velocity is controlled by parameters other than distance of meteor from camera, the image velocity will be treated as directly proportional to the product of velocity of the meteor relative to the atmosphere and a function of the zenith angle $F_v(Z_R)$. That function will be understood as also a function of height of the meteor above ground level h_g , azimuth of the meteor path, and position of the meteor within camera field of view. At the same time, the image velocity will be treated as inversely proportional to the distance of the meteor from the camera. Again, distance of meteor from camera will be treated as proportional to h_g and F_h . Accordingly,

$$v_i \propto v F_v(Z_R) h_g^{-1} F_h^{-1} \quad (6)$$

where v is instantaneous meteor velocity relative to the atmosphere. For the present $F_v(Z_R)$, like F_h earlier, may be regarded as an arbitrary correction factor which will be given such value as necessary for each meteor in order to make proportionality (6) correct. Its use at this stage avoids complications involving position within field of view, which can well be left till later.

From proportionalities (4), (5), and (6), the expression for photographic exposure becomes

$$E \propto I_m v^{-1} h_g^{-1} F_h^{-1} F_v(Z_R)^{-1} \quad (7)$$

Effective Exposure

Proportionality (7) does not express exactly the effective exposure upon a photographic emulsion because of the effect known as reciprocity failure. This effect is a measure of the failure of the photographic emulsion to comply with the so-called reciprocity law. According to that law, the photographic density or darkening of the emulsion should depend only upon photographic exposure as defined by equation (3) regardless of values of image brightness and exposure duration individually.

The manufacturer of the emulsion used for the photographs of reference 2 has provided data regarding reciprocity failure, for marginal photographic density, for exposure durations only as low as $10^{-2.4}$ second. The exposure durations in meteor photography are understood to have been substantially lower, of the order of 10^{-6} to 10^{-4} second. The reciprocity failure for marginal photographic density, however, is substantially constant in the region from $10^{-1.5}$ to $10^{-2.5}$ second. That is, for constant and barely visible photographic density in the region of values of T from $10^{-1.5}$ to $10^{-2.5}$ second, a linear relation exists between $\log IT$ and $\log I$. Hence, under an assumption that this relation will not rapidly become nonlinear, extrapolation to the region applicable in the meteor photography may provide a better approximation than complete neglect of reciprocity failure.

According to the manufacturer's data, the same just visible density is obtained with

$$\left. \begin{aligned} \log_{10} I_1 T_1 &= -1.8 \\ \log_{10} I_1 &= -0.5 \end{aligned} \right\} \quad (8)$$

as with

$$\left. \begin{aligned} \log_{10} I_2 T_2 &= -1.76 \\ \log_{10} I_2 &= 0.6 \end{aligned} \right\} \quad (9)$$

where I_1 and I_2 are intensities of illumination of emulsion, and T_1 and T_2 are exposure durations. By extrapolation, throughout the region from 10^{-6} to about $10^{-1.5}$ second, the same slope m_s on a log-log plot will be assumed as is indicated by equations (8) and (9). That is,

$$m_s = \frac{\log_{10} I_2 T_2 - \log_{10} I_1 T_1}{\log_{10} I_2 - \log_{10} I_1} \quad (10)$$

From equations (8) to (10),

$$m_s = 0.03636 \quad (11)$$

Now it is desired to derive a function E_{eff} , termed effective exposure, which will remain constant under the conditions expressed by equations (8) to (11). Such a function may be expressed as

$$E_{\text{eff}} \propto IT^\psi \quad (12)$$

where ψ is a constant. From equation (10),

$$I_1 T_1^{1/(1-m_s)} = I_2 T_2^{1/(1-m_s)} \quad (13)$$

Equation (13) shows that proportionality (12) will be satisfied if

$$E_{\text{eff}} \propto IT^{1/(1-m_s)} \quad (14)$$

or

$$E_{\text{eff}} \propto I_i T^{1.038} \quad (15)$$

Comparison of proportionality (15) with equation (3) and review of proportionalities (4) to (7) show that consideration of reciprocity failure will convert proportionality (7) to

$$E_{\text{eff}} \propto I_m v^{-1.038} h_g^{-0.962} F_h^{-0.962} F_v(Z_R)^{-1.038} \quad (16)$$

or

$$E_{\text{eff}} = k_1 I_m v^{-1.038} h_g^{-0.962} F(Z_R)^{-1} \quad (17)$$

where k_1 is a constant that does not need to be evaluated and

$$F(Z_R) = F_h^{0.962} F_v(Z_R)^{1.038} \quad (18)$$

Atmospheric Density for Maximum Effective Exposure

The meteoroid altitude for maximum effective exposure will be sought now. The atmospheric density for maximum effective exposure is determined as an intermediate step, by a method closely analogous to that used by Hawkins and Southworth (ref. 9) in which they determined atmospheric density corresponding to the time of maximum meteor luminosity. Such luminosity was intrinsic and not necessarily directly related to effective photographic exposure under all conditions. As in reference 9, the effect of meteor fragmentation is ignored. Justification for doing so will be discussed later.

The following intensity equation, derived in reference 9, is used:

$$I_m = \frac{\Lambda A m^{2/3}}{4 \zeta \rho_m^{2/3}} \tau \rho v^5 \quad (19)$$

where Λ is efficiency of utilization of kinetic energy in the ablation of mass, A is particle shape factor, m is instantaneous particle mass, ζ is the energy required to ablate one unit mass of a particle, ρ_m is density of the meteor particle, τ is the luminous efficiency, approximately the fraction of lost kinetic energy of the meteoroid that is converted to photographable radiation, and ρ is instantaneous air density. From proportionality (17) and equation (19),

$$E_{\text{eff}} = k_2 m^{2/3} \rho h_g^{-0.962} \quad (20)$$

where

$$k_2 = \frac{k_1 \Lambda A \tau v^{3.962} F(Z_R)^{-1}}{4 \xi \rho_m^{2/3}} \quad (21)$$

In accordance with customary practice, the particle velocity v is treated as a constant. Such treatment is justified from a practical standpoint because observed loss of velocity of meteors throughout their entire paths is usually very small. The factor k_2 defined by equation (21) is a grouping of entities that may be combined for the present, for simplicity, and which may be regarded as substantially constant relative to time for a particular meteor.

At this point, a desirable procedure would be to express h in equation (20) in terms of ρ and to differentiate equation (20), thereby obtaining an expression for air density at the maximum value of E_{eff} . It is well known that atmospheric air density varies approximately as the following function of altitude above sea level (ref. 10),

$$\rho = \rho_0 e^{-h/H} \quad (22)$$

where ρ_0 is a constant and H is scale height, or the difference in altitude corresponding to an air density ratio of e^{-1} in the atmosphere. Equation (22) can be solved for altitude above sea level h and corrected for altitude h_g . The result can be substituted into equation (20). The result, however, is not convenient for differentiation and subsequent solution.

Appendix B shows that the relation between air density and altitude above sea level can be expressed approximately, throughout the altitude range practically concerned with meteors, by the equation,

$$h = k_3 \rho^{-0.0627} \quad (23)$$

where k_3 is a constant. As no large percentage error results, the height above ground level h_g may be taken as equal to the altitude above sea level h . Accordingly, from equations (20) and (23),

$$E_{\text{eff}} = k_4 m^{2/3} \rho^{1.060} \quad (24)$$

where

$$k_4 = \frac{k_2}{(k_3)^{0.962}} \quad (25)$$

From equation (24), with differentiation relative to time,

$$\frac{d}{dt} (\log E_{\text{eff}}) = \frac{2}{3m} \frac{dm}{dt} + \frac{1.060}{\rho} \frac{d\rho}{dt} \quad (26)$$

Thus, for maximum effective exposure,

$$\frac{1.060}{\rho} \frac{d\rho}{dt} = - \frac{2}{3m} \frac{dm}{dt} \quad (27)$$

The left-hand side of equation (27) can be evaluated with the more accurate relation expressed by equation (22) and with the obvious relation

$$\frac{dh}{dt} = -v_{\infty} \cos Z_R \quad (28)$$

where v_{∞} is velocity of the meteoroid (the particle that produces the meteor) before any deceleration has been caused by the atmosphere. The right-hand side may be evaluated with use of an energy equation derived in reference 9:

$$\zeta \frac{dm}{dt} = -\frac{1}{2} \Lambda A \rho_m^{-2/3} m^{2/3} \rho v^3 \quad (29)$$

where

dm/dt is the rate of mass ablation, which conventionally is always negative. Accordingly, from equations (22) and (27) to (29), with v constant and therefore equal to v_{∞} , the air density for maximum effective exposure is

$$\rho_{\text{m.e.}} = \frac{3.18 \rho_m^{2/3} m_{\text{m.e.}}^{1/3} \zeta \cos Z_R}{\Lambda H A v_{\infty}^2} \quad (30)$$

where $m_{\text{m.e.}}$ is the remaining mass of the meteoroid at the time of maximum effective exposure.

Equation (30) expresses the desired value of atmospheric density at maximum effective exposure, but with the fault that it contains the parameter $m_{\text{m.e.}}$. For that reason, the desired atmospheric density is not expressed solely as a function of the meteoroid characteristics at the time of arrival of the meteoroid at the upper limits of the atmos-

phere. Hence, elimination of $m_{m.e.}$ from equation (30) is now desired. Hawkins and Southworth (ref. 9) integrated equation (29) and developed an equation interrelating meteoroid mass to altitude which is valid for this purpose:

$$m^{1/3} = m_{\infty}^{1/3} + \frac{\Lambda A v_{\infty}^2}{6 \xi \rho_m^{2/3} \cos Z_R} \int_{+\infty}^h \rho \, dh \quad (31)$$

where m_{∞} is the initial mass of the meteoroid.

From equation (22), the integral in equation (31) may be evaluated for the altitude at maximum effective exposure $h_{m.e.}$ to yield

$$m_{m.e.}^{1/3} = m_{\infty}^{1/3} - \frac{H \Lambda A v_{\infty}^2 \rho_{m.e.}}{6 \xi \rho_m^{2/3} \cos Z_R} \quad (32)$$

Substitution of $\rho_{m.e.}$ from equation (30) into equation (32) gives the following expression for mass at maximum effective exposure:

$$m_{m.e.}^{1/3} = 0.654 m_{\infty}^{1/3} \quad (33)$$

From equations (30) and (33),

$$\rho_{m.e.} = \frac{2.080 \rho_m^{2/3} m_{\infty}^{1/3} \xi \cos Z_R}{\Lambda H A v_{\infty}^2} \quad (34)$$

Expression for Maximum Effective Exposure

The value of maximum effective exposure may be obtained readily from equations (21), (24), (25), (33), and (34). If v_{∞} is substituted for v in equation (21), the value of k_2 from equation (21) is substituted into equation (25), and subsequently the value of k_4 from equation (25) is substituted into equation (24), equation (24) becomes

$$E_{\text{eff(max)}} = \frac{\Lambda A \tau v_{\infty}^{3.962} F(Z_R)^{-1} k_1}{4 \xi \rho_m^{2/3} k_3^{0.962}} m^{2/3} \rho^{1.060} \quad (35)$$

If $m_{m.e.}$ from equation (33) is substituted for m and $\rho_{m.e.}$ from equation (34) is substituted for ρ in equation (35), equation (35) becomes

$$E_{\text{eff(max)}} = \frac{\Lambda A \tau v_{\infty}^{3.962} F(Z_R)^{-1} k_1}{4 \zeta \rho_m^{2/3} k_3^{0.962}} (0.654)^2 m_{\infty}^{2/3} \left(\frac{2.080 \rho_m^{2/3} m_{\infty}^{1/3} \zeta \cos Z_R}{\Lambda H A v_{\infty}^2} \right)^{1.060} \quad (36)$$

Opinions of authoritative sources are not unanimous concerning the relation of luminous efficiency to velocity (refs. 6, 11, and 12). Verniani's conclusion (ref. 12), which will be used here, appears to agree more closely with Öpik's as found in reference 11 than as found in reference 6. It is expressed by

$$\tau = \tau_0 v \quad (37)$$

where τ_0 is a constant. As will be observed later, use of some exponent other than unity for v in equation (37) would not affect the correction factor derived in this work, for it is based upon an empirically determined exponent of v_{∞} . With substitution of τ from equation (37), equation (36) expresses $E_{\text{eff(max)}}$ as a product of four basic parameters, v_{∞} , m_{∞} , $\cos Z_R$, and $F(Z_R)$, to various positive or negative powers multiplied by numerous factors that are not functions of those four parameters. The factors that are not functions of the four basic parameters may be grouped together as one term, which does not need to be evaluated, namely,

$$k_5 = \frac{1}{4} (0.654)^2 \left(\frac{2.080}{H} \right)^{1.060} \left(\frac{\zeta \rho_m^{2/3}}{\Lambda A} \right)^{0.060} \tau_0 \frac{k_1}{k_3^{0.962}} \quad (38)$$

Equation (36), then, becomes

$$E_{\text{eff(max)}} = k_5 m_{\infty}^{1.020} v_{\infty}^{2.842} (\cos Z_R)^{1.060} F(Z_R)^{-1} \quad (39)$$

Equation (39) expresses relative values of the greatest effective exposures that are reached at any time, for different meteors, in terms of three important basic parameters describing conditions at arrival of the meteoroids at the outer limits of the atmosphere. Those basic parameters are meteoroid mass m_{∞} , meteoroid velocity relative to the atmosphere v_{∞} , and angle of meteoroid path to the zenith Z_R . The relation to the zenith angle Z_R is complicated by the presence of the function $F(Z_R)$, which is discussed in appendix C.

Theoretical Criterion for Marginal Photographic Density

As a final step in the theoretical effort of stage 1, it is necessary to arrive at a theoretical criterion for marginal photographic exposure. As the maximum effective exposure developed at any time by a meteor controls whether a trace may be discovered in visual examination of the plates, the maximum effective exposure is identical with marginal exposure if the photographic trace is just barely visible. Hence, under the condition of marginal exposure, $E_{\text{eff(max)}}$ of equation (39) must have exactly some specific value as yet undetermined.

Now the factor k_5 contains only parameters ρ_m and A that may vary from meteor to meteor. Their variation, moreover, should not be important statistically in the applications for which the end result of this study is intended. Therefore, the fraction $E_{\text{eff(max)}/k_5$ also must have exactly some specific value in order that marginal exposure may exist.

Thus, the desired theoretical criterion for marginal exposure may be written from equation (39) as

$$C_{\text{marg}} = \frac{E_{\text{eff(max)}}}{k_5} = m_{\infty}^{1.020} v_{\infty}^{2.842} (\cos Z_R)^{1.060} F(Z_R)^{-1} \quad (40)$$

A determination of the magnitude of C_{marg} is not necessary because for this study only the exponents appearing in the right-hand side of equation (40) are needed. An empirical study of the correct values of those exponents will be undertaken next. Assignment of a more specific significance to the function $F(Z_R)$ will be considered when the need arises. Equation (40) is the end result of the theoretical part of stage 1 of this study as earlier described. The empirical part of stage 1 of the study will now be undertaken.

EMPIRICAL CRITERION FOR MARGINAL PHOTOGRAPHIC DENSITY

Empirical support for or revision of equation (40) as a criterion for the existence of marginal photographic exposure is desirable at this point, for the following reasons: A number of minor uncertainties existed in the theoretical development of equation (40). The total effect of those uncertainties might prove to be substantial. To the extent such uncertainties affect the exponents in equation (40) rather than its basic form, a lump correction can be applied for all the uncertainties on an empirical basis. When the best such lump correction has been found, then the basic form of the equation may be judged empirically by the consistency of the results and the quality of correlations it produces.

Particular importance attaches to the establishment of accurate values for the exponents in equation (40) because in the next stage of the development of an adjusting factor for simultaneous correction of mass and velocity bias, small errors in the exponents would become magnified.

Some of the uncertainties that may be corrected by an empirical revision of equation (40) are as follows:

The basic equations from which equation (40) was derived are to a considerable extent theoretical rather than empirical. Extrapolation was necessary in the treatment of reciprocity failure. The function $F(Z_R)$ can be defined, from the information provided in reference 2, only on a statistical basis, involving some uncertainty. The argument is given in appendix D that fragmentation should cause a random departure from the value of $E_{\text{eff(max)}}$ computed with use of equation (39) and that such departure should be within satisfactory limits for statistical purposes. The random nature of this effect and its relative importance need to be confirmed empirically.

Reason exists to suspect that marginal photographic density on the photographic emulsion may not be a perfect criterion for the discovery of a meteor trail. Because of the action of a rotating shutter in each of the cameras, a meteor trail was photographed as a series of dashes. For lower image velocities, these dashes are shorter than for higher. As the photographs of the meteor trails are imbedded in a dense background of star images, there may be some danger of failure to observe meteor trails in cases where the individual dashes are very short. If the length of an individual dash is less than the diameter of the circle of confusion of a point image on the plate, the density of the developed trace on the plate will be reduced, and failure to discover the trace may be even greater. Such failure, from either cause, amounts to a bias against the discovery of slow moving meteoroids not taken into account in the derivation of equation (40).

Before an empirical evaluation of equation (40) can be made, a calculable significance must be assigned to the function $F(Z_R)$. Such a significance could be defined readily for each meteor in terms of zenith angle and position of the meteor within the field of view. However, positions of meteors within the field of view were not included within the data published in reference 2 by McCrosky and Posen. Moreover, the results of this study were intended specifically for application to the meteor data reported in that reference.

For those reasons, the function $F(Z_R)$ has been calculated as a statistically expected value for each meteor $F(Z_R)_{\text{av}}$ and as a minimum value for each meteor $F(Z_R)_{\text{min}}$ in a manner that takes into account many sample positions within the field of view as described in appendix C. In such calculations, the angle of the meteor path to the zenith was used as given in reference 2. Use was also made of a value of azimuth of the meteor path as determined from data given in reference 2.

Discussions of various matters concerned with the function $F(Z_R)$ appear in appendix E.

Method of Testing Criterion for Marginal Meteoroid Trails

In the choice of a procedure for testing the validity of equation (39) or equation (40), consideration must be given to the fact that equation (40) will be used later as a criterion for existence of marginal effective exposure. The equation will not be used in reference to meteors providing effective exposures greater than marginal. Hence, any possible modification of equations (39) and (40) according to the most consistent results obtained in application to all meteors would be less desirable than modification to provide the most consistent result in application to meteors that produced marginal photographic densities. Of particular importance here is the fact that use of meteors of marginal photographic density, if chosen on the basis of the actual success in their discovery, should take into account the earlier mentioned bias against discovery of slow moving meteors because of the background of star trails. Checking equations (39) and (40) by application to the data for all meteors would not provide this advantage.

Consequently, a decision was made to select a set of meteors all of which were believed to have produced approximately marginal photographic density. After such a set of meteors was selected, equation (40) could be applied to the data given for those meteors in reference 2, with various substitute values for the exponents. The best set of substitute exponents, and the intrinsic merit of equation (40) with that best set of exponents, could then be judged by the uniformity of the values of C_{marg} determined. Meteors chosen should cover a wide range of combinations of mass, velocity, and zenith angle to provide the best test. The method of selection of such a set of meteors follows.

Selection of Meteor Trails of Marginal Density

Meteor trails that produced approximately marginal photographic density selected from the data of reference 2 will be termed "test meteors". Data given in reference 2 that were used for their selection, with the symbols used in that reference, are (1) photographic magnitude M_{pg} , adjusted to a standard distance of 100 kilometers and, in effect, to a standard velocity; (2) height in kilometers above sea level at beginning of trail H_B ; (3) meteoroid velocity relative to the atmosphere in kilometers per second v_∞ ; (4) cosine of the zenith angle CZ_R ; (5) number of shutter breaks in meteor trail n ; and (6) the time interval between shutter breaks, 0.0167 second.

The method of selection of 100 test meteors will be specified in detail; then, how

such method of selection provides the desired characteristics for the set of test meteors will be explained. The test meteors were chosen among 2021 of the sporadics reported in reference 2 in the following manner:

(1) Ten velocity (v_{∞} in ref. 2) classes were chosen, each containing as nearly as possible the same number of meteors but with all boundaries between adjacent classes exactly midway between two consecutive integral values of velocity in kilometers per second.

(2) Within each velocity class, 10 zenith-angle (CZ_R in ref. 2) subclasses were chosen with as nearly as possible equal content. As only two significant figures were used in reporting the values of $\cos Z_R$ (CZ_R in ref. 2), absolute equalization of the count within different subclasses was not possible without placing meteors of the same reported zenith angle in each of two adjacent subclasses. Hence, unequal contents of subclasses were permitted to the extent necessary.

(3) For each meteor, the height for maximum effective exposure was taken as the height at the end of the trail, which was determined from the equation

$$h_{m. e.} = H_B - 0.0167 n v_{\infty} \cos Z_R \quad (41)$$

(4) The photographic magnitude reported for each meteor was adjusted for height and meteor velocity according to the following equation to obtain a magnitude expressing conditions on the photographic plates

$$M_{adj} = M_{pg} + 2.5 \log_{10}(h_{m. e.} v_{\infty}) \quad (42)$$

(5) From each of the 100 subclasses resulting from items (1) and (2), the two meteors having the greatest values of M_{adj} were chosen.

(6) The possibly serious effect of any gross errors on the high side in the reporting of values of M_{pg} in reference 2 was minimized by rejecting the meteor having the greatest value of M_{adj} in each subclass.

(7) The remaining 100 meteors, those having the second greatest values of M_{adj} in the various subclasses, were taken as the desired test meteors.

In the selection process described, the use of 2021 meteors as a base resulted from the exclusion of all meteors for which masses were not reported and all meteors for which $\cos Z_R$ was less than 0.2. Exclusion of the meteors with $\cos Z_R$ less than 0.2 was necessary because of the sensitivity of equation (40), throughout the region of small values of $\cos Z_R$, to small errors in that function. In particular, equation (40) can not yield a realistic value of C_{marg} when $\cos Z_R$ equals zero. As nine meteors are reported in reference 2 with $\cos Z_R$ equal to zero, a minimum cutoff point was essential.

The value 0.2 resulted in exclusion of 18 meteors; only about 0.9 percent of the total of 2039 that would otherwise have been included.

The determination of height for maximum effective exposure with equation (41) represented merely the best that could be done in the absence of better information. Figure 5 of appendix B shows that the total vertical component of length of meteors of marginal photographic density was usually less than 10 kilometers. Hence, any inaccuracy of this treatment should not cause a large percentage of error.

The effective standard velocity for which values of M_{pg} were adjusted by the authors of reference 2 could be deduced from information given by Whipple and Jacchia in reference 13. For the intended use of the value of M_{adj} from equation (42), however, inclusion of this value was pointless. The standard altitude of 100 kilometers was also omitted from equation (42). The equation consequently yielded values of M_{adj} quite unrealistic except for the comparative purpose intended.

The adjustment for height and velocity provided by equation (42) is not related to the effect of these parameters in equation (40). Instead, equation (42) merely removed two adjustments made by the authors of reference 2 in the values of M_{pg} reported by them because those adjustments are not desirable for the present purpose. Equation (42) removes those adjustments accurately, for comparative purposes, only when applied to meteors within a narrow range of zenith angle and only under the condition, discussed in appendix E, that the meteor of maximum magnitude within a subclass should have occurred near the field position most favorable from the standpoint of discovery of a meteor trail. That is, equation (42) is applicable only within a particular subclass of meteors from which a test meteor is to be chosen.

Obviously the selection method described satisfied the desirable condition that the test meteors should cover a wide range of combinations of values of v_{∞} and $\cos Z_R$. Also, the condition of approximately marginal photographic density should be met, because each test meteor selected was the second faintest within its subclass. For a large subclass, the two faintest meteors should each involve a photographic density barely sufficient to permit their discovery. The content of the subclass should not need to be very great because it is well known that the frequency of occurrence of meteors increases rapidly with increasing magnitude. The desirable condition of a wide range of values of m_{∞} should also be met by the method of selection described, for substantial variations of m_{∞} would be needed to provide uniformly marginal photographic density with the widely varying values of v_{∞} and $\cos Z_R$. The relation of the selection process described to the function $F(Z_R)$ is discussed in appendix E.

Serial numbers of the 100 meteor trails selected by the method just described, with various pertinent data, are shown in table I. The page and line numbers are shown for locations of these meteor data in reference 2. The values as obtained from reference 2 are shown for M_{pg} , m_{∞} , $\cos Z_R$, and v_{∞} . Also shown are the value of M_{adj} com-

puted with equation (42) and values of $F(Z_R)_{\min}$ and $F(Z_R)_{\text{av}}$, which are explained in appendixes E and C. The serial number of the rejected meteor within each subclass having the greatest value of M_{adj} is also given with its value of M_{adj} . In addition, table I shows the lower and the upper limits of v_{∞} for each velocity class, the lower and the upper limits of $\cos Z_R$ for each zenith-angle subclass, and the number of meteors within each subclass.

Comparison of Computed Effective Exposures for Various Meteor Trails

If equation (40) is valid and if the meteors listed in table I actually did produce photographic records of marginal and consequently uniform density, then application of equation (40) to the data for those meteors should produce uniform values of C_{marg} .

The values of M_{adj} are not exactly uniform. The average value is 10.295, with a standard deviation of 0.369. Such a degree of nonuniformity may be due principally to four effects: (1) random variations in the lower limit of density that observers were able to discover in examining the plates, (2) random variations in the closest approach to the most favorable field position within the various subclasses (appendix E), (3) the fact that equation (42) is not strictly applicable from one subclass to another, and (4) the relation of the uniformity of maximum magnitudes within various subclasses to sizes of those subclasses.

At this point, to determine which cause predominates is not possible except that a progressive variation probably due to cause (3) is fairly obvious. Hence, the variation in values of M_{adj} can not be assumed to be a measure of variation of photographic densities. However, because of the variation in values of M_{adj} , a commensurate variation in values of C_{marg} from equation (40) would not be inconsistent with valid applicability of equation (40) for its intended purpose.

The effects of fragmentation and other uncertainties involved in the development of equation (40), as listed earlier, could cause an even greater variation in values of C_{marg} . Such uncertainties would tend to do so particularly to the extent that they involve a degree of randomness. But if the variation in values of C_{marg} should be only moderately greater than the variation in values of M_{adj} , such moderate excess variation should indicate a limiting magnitude for all the random effects of the uncertainties involved in the development of equation (40).

The task is now set to apply an equation in the form of equation (40) to the data for each of the 100 test meteors for two purposes: (1) to determine the relative values of the four exponents in that equation which produce the most nearly uniform values of C_{marg} and (2) to compare the variation in those most nearly uniform values with the variation in values of M_{adj} of table I, with the object of deciding whether the value of C_{marg}

according to equation (40) is a satisfactory criterion for marginal photographic density.

A computer program was used to apply the following equation to the data for the 100 test meteors shown in table I, with various combinations of values of the three variable exponents, and to indicate the degree of uniformity of the resulting values of C_{marg} for each such combination:

$$C_{\text{marg}} = m_{\infty}^{1.02} v_{\infty}^{\mu} (\cos Z_R)^{\nu} F(Z_R)^{-\xi} \quad (43)$$

Equations (40) and (43) are identical except that three exponents have been made variable in equation (43). Constancy of the exponent of m_{∞} will be discussed later. A combination of values of μ , ν , and ξ was sought which would produce the most uniform results and thereby confirm equation (40), if the values of μ , ν , and ξ should agree with the exponents in equation (40), or which otherwise would provide an empirical improvement of equation (40) by substitution of new values for one or more of the three exponents.

For a given combination of exponents, and with substitution of $F(Z_R)_{\text{min}}$ of table I for $F(Z_R)$ for reasons explained in appendix E, the following procedure was used:

- (1) A value of C_{marg} was computed with equation (43) for each test meteor.
- (2) The results of item (1) were converted to natural logarithms.
- (3) The mean value of logarithms from item (2) was found.
- (4) The total of the squares was obtained for the differences between the individual logarithms from item (2) and the mean value from item (3).
- (5) The result from item (4) was divided by 100, the number of test meteors, and was reported out by the computer as a variance (square of the standard deviation).

Hence, the value of variance shown by the computer for a given combination of values of μ , ν , and ξ was

$$V_{\mu, \nu, \xi} = \frac{1}{100} \sum_{i=1}^{100} \left[\left(\log_e C_{\text{marg}} \right)_i - \left(\log_e C_{\text{marg}} \right)_{\text{av}} \right]^2 \quad (44)$$

where the subscript i refers to a particular test meteor, and the expression $\left(\log_e C_{\text{marg}} \right)_{\text{av}}$ represents the average value of the logarithm of C_{marg} as computed for the 100 test meteors.

As indicated by equation (43), in the selection of combinations of values of exponents the exponent of m_{∞} was always given the value 1.020 as in equation (40). Fixation of one of the four exponents in advance was necessary because any proportional reduction of all four exponents would reduce the variance produced by equation (44). Hence, any attempt to minimize the variance by adjustment of all four exponents would lead to the trivial indication that the most uniform result is obtained with all exponents equal to

zero. No strong case can be made for selection of the exponent of m_∞ as a constant in preference to the other exponents in equation (43). However, the minimum value of variance from equation (44) would be obtained with the same proportionality between the four exponents, regardless of which exponent was held constant or at what level. Moreover, if equation (43) is valid with a given set of four exponents, it must be equally valid when all those exponents are multiplied by one and the same constant.

The significant results of this procedure are presented in figures 1 to 3.

Each curve in figure 1 shows the relation of $V_{\mu, \nu, \xi}$ to μ for a constant combination of values of ν and ξ . For each part of the figure, the value of ξ is constant, but ξ varies between one part of the figure and another. Each plotted point represents a computer result with use of equations (43) and (44) for a discrete set of values of μ , ν , and ξ . The faired curves were constructed solely on the basis of the locations of the plotted discrete points.

The 20 discrete points in figure 2 show the minimum value of $V_{\mu, \nu, \xi}$ reached by each of the 20 faired curves in the four parts of figure 1, plotted against the value of ν for each such curve, without regard to the various values of μ at which such minimums occurred. The faired curves in figure 2 were constructed solely on the basis of the discrete points plotted in that figure. Each such faired curve represents a constant value of ξ .

In figure 3, the four discrete points represent the minimum value of $V_{\mu, \nu, \xi}$ reached by each of the faired curves in figure 2, plotted against the value of ξ for each such curve, without regard to the values of μ and ν associated with the various minimums. The faired curve in figure 3 was constructed solely on the basis of the discrete points plotted in that figure.

Figures 1 to 3 indicate 0.2801 as the lowest value of $V_{\mu, \nu, \xi}$ that can be obtained. Values of 2.93, -0.19, and 0.54 for μ , ν , and ξ may be estimated from the figures, with suitable interpolations, as being associated with this minimum variance. Accordingly, a single rerun of the computer program was executed to check the value of $V_{2.93, -0.19, 0.54}$ according to equation (44) and to compute the value of C_{marg} according to equation (43) for each of the 100 test meteors.

The value of $V_{2.93, -0.19, 0.54}$ resulting from that computer run was 0.2802, virtually the same as predicted. The computed values of C_{marg} are plotted in figure 4 in four orders as follows: (1) ascending values of v_∞ , (2) ascending values of m_∞ , (3) ascending values of $\cos Z_R$, and (4) ascending values of $F(Z_R)_{\text{min}}$. The generally horizontal trend of each of the four plottings in figure 4 confirms the values of μ , ν , and ξ shown by figures 1 to 3. The virtual absence of systematic waves or portions of waves in the four plottings supports the theoretically developed equation (43) in its indication that C_{marg} should be proportional to powers of v_∞ , m_∞ , $\cos Z_R$, and $F(Z_R)_{\text{min}}$.

The plotting in order of ascending values of m_∞ does show a tendency toward

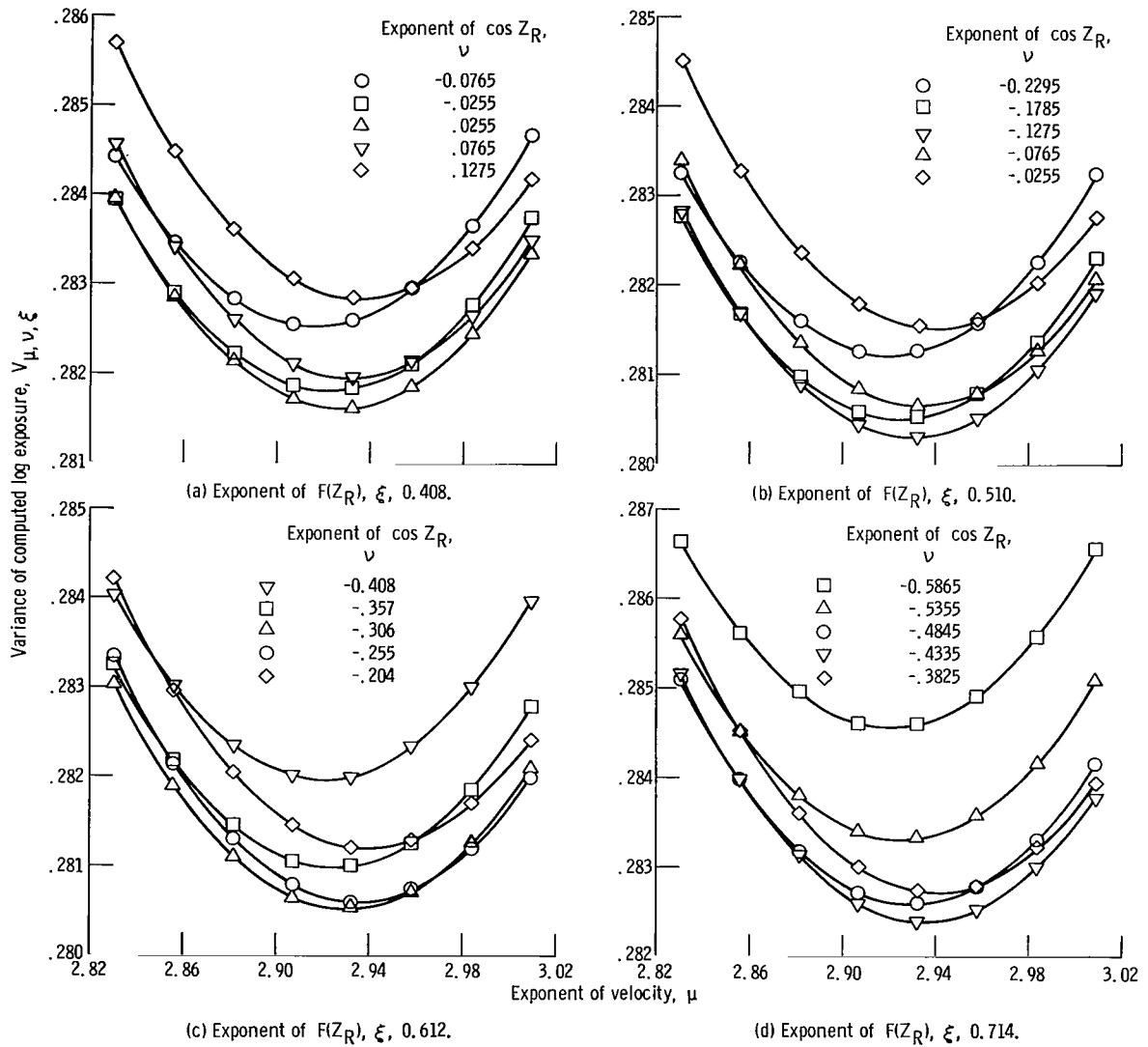


Figure 1. - Variance of logarithm of computed effective exposure related to exponent of meteoroid velocity relative to atmosphere; Z_R is zenith angle.

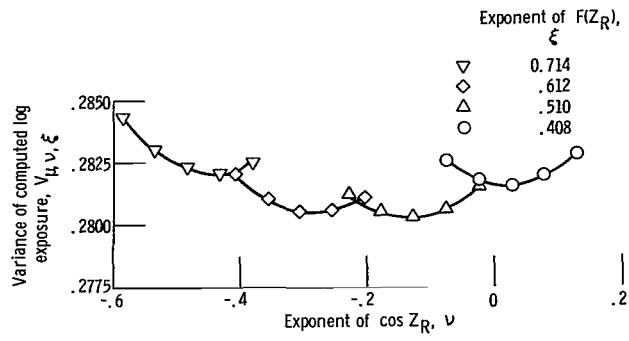


Figure 2. - Variance of logarithm of computed effective exposure related to exponent of cosine of zenith angle Z_R .

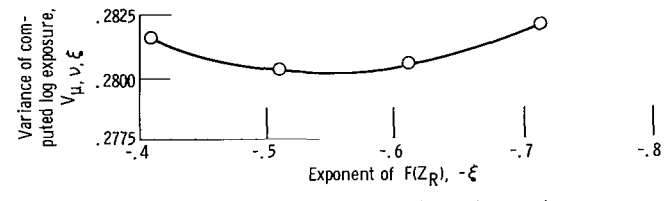


Figure 3. - Variance of logarithm of computed effective exposure related to exponent of function of zenith angle, Z_R .

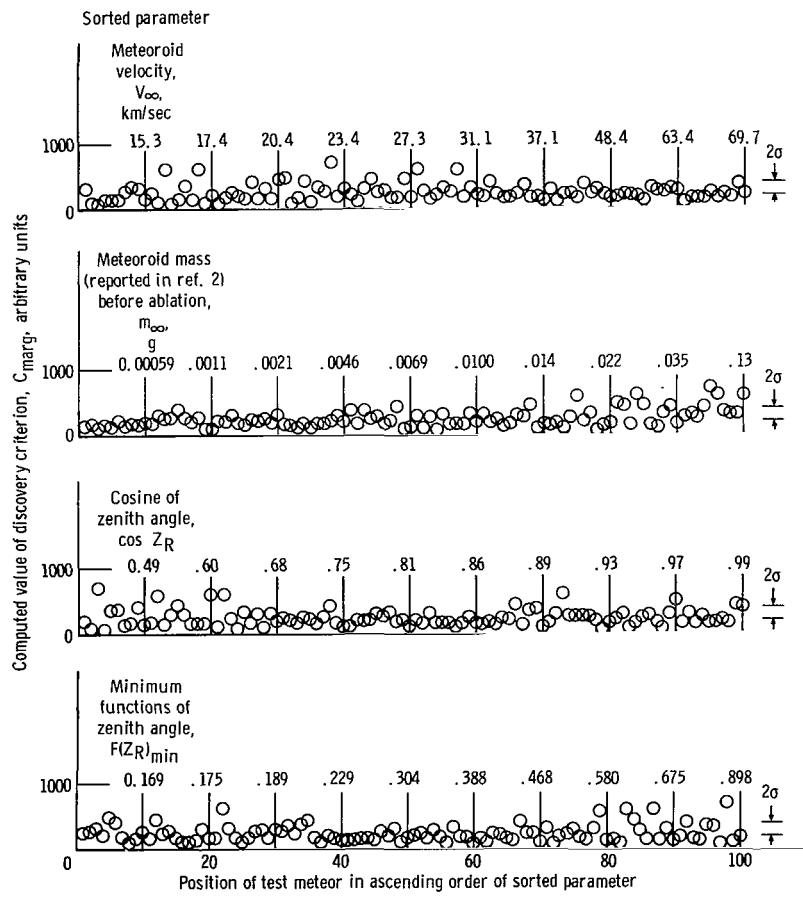


Figure 4. - Computed values of discovery criterion arranged in various orders; $\sigma = (V_{2, 93, -0.13, 0.54})^{1/2}$.

higher computed values of C_{marg} at the greater values of m_{∞} . The same higher values of C_{marg} tend to appear at the left side of the plotting in order of ascending values of $\cos Z_R$. However, all four plottings in figure 4 are believed to be so flat as to support equation (43) adequately for the purpose of the present analysis, with the values 2.93, -0.19, and 0.54 for μ , ν , and ξ . Introducing complications into the equation for the purpose of flattening the plottings further is not believed to be justified.

The results as illustrated in figures 1 to 3, therefore, indicate that equation (40) on an empirical basis becomes

$$C_{\text{marg}} = m_{\infty}^{1.020} v_{\infty}^{2.93} (\cos Z_R)^{-0.19} F(Z_R)_{\text{min}}^{-0.54} \quad (45)$$

Appraisal of Revised Criterion for Discovery of Image Trail

In the preceding section, equation (40), theoretically derived, was changed empirically to equation (45) by revision of the values of three exponents with use of $F(Z_R)_{\text{min}}$ for $F(Z_R)$. The new exponent of v_{∞} agrees with the derived value within 3.1 percent. The new exponents for $\cos Z_R$ and $F(Z_R)$ differ drastically from the theoretically derived values.

Part of the purpose of the empirical study was to provide any necessary adjustment for the subjective difficulty in discovery of slow moving meteors. Superficially, the close confirmation of the exponent of v_{∞} might be thought to repudiate the existence of this subjective difficulty. However, it may be that the close confirmation of the exponent of v_{∞} is an accidental result of two mutually compensating effects: (1) the maximum effective exposure varies basically as a power of v_{∞} somewhat less than that which was theoretically derived and (2) the subjectively greater ease of discovery of a fast moving meteor on the photographic plate calls for an increase in the power of v_{∞} in order to make C_{marg} of equation (45) a true discovery criterion rather than a criterion for a definite level of maximum effective exposure.

At first sight, the change in sign of the exponent of $\cos Z_R$ seems to repudiate the theoretical result entirely. Such is not really the case, however, because the function $F(Z_R)_{\text{min}}$ contains implicitly as a factor a negative power of $\cos Z_R$. The interrelations of $\cos Z_R$, $F(Z_R)_{\text{min}}$, and $F(Z_R)_{\text{av}}$ involved in an appraisal of equation (45) are discussed in appendix E. It is argued there that equation (45), for application to any meteor rather than to each of the 100 test meteors, should be changed to

$$C_{\text{marg}} = m_{\infty}^{1.02} v_{\infty}^{2.93} (\cos Z_R)^{0.167} F(Z_R)_{\text{av}}^{-0.54} \quad (46)$$

The reduction of the exponent of $\cos Z_R$ from the value 1.060 in equation (40) to

the value 0.167 in equation (46) is not necessarily disturbing. The factor $(\cos Z_R)^{1.060}$ in equation (40) represents the tendency of an obliquely descending meteor to produce its maximum effective exposure at a higher altitude than a meteor that descends more nearly vertically. But the derivation of the factor neglected the effect of fragmentation. Fragmentation is known to occur frequently with the faint meteors involved in this study (ref. 14). As shown in appendix D, late fragmentation generally should cause much greater increase of effective exposure than early fragmentation. A possible tendency of early fragmentation to occur with small zenith angles and of later fragmentation to occur with larger zenith angles might tend to offset the more direct effect of zenith angle on maximum exposure, with the result that the exponent of the cosine of the zenith angle in equation (40) should be reduced.

The minimum variance of 0.2802 in the natural logarithm of the computed discovery criterion C_{marg} amounts to a standard deviation of approximately 0.57 magnitude. This result compares favorably with the standard deviation of 0.369 mentioned earlier in the values of M_{adj} for the 100 test meteors. The increase of approximately 0.2 magnitude in the standard deviation is within the range that might be expected on the basis of the discussion of the effect of fragmentation in appendix D.

From the foregoing discussion, C_{marg} of equation (45) appears to be adequately supported as a discovery criterion. The differences between that equation and equation (40) appear to be no greater than might reasonably be expected because of a possibly systematic effect of fragmentation and other effects that have been discussed. The standard deviation in values of C_{marg} is quite reasonable. In appendix E, equation (46) is shown to be virtually equivalent to equation (45) and theoretically should be slightly better for application to all meteors.

At this point, empiricism must be given precedence over theoretical deduction, and equation (46) will be taken as applicable rather than equation (40). The entire right-hand side of equation (46) might be raised to a positive power greater or less than unity if the correct exponent of m_∞ should later be found to be other than 1.02, but the relative effect of C_{marg} as a discovery criterion would be unchanged. Nothing in the present analysis gives empirical support to the absolute values of the exponents. The empirical support applies only to the ratios of those exponents to each other. Moreover, equation (46) is now a discovery criterion rather than a criterion for a particular level of effective exposure. And equation (46) has been supported empirically only for the photographic equipment and for conditions that existed for the photographs reported in reference 2. Such support would not necessarily apply for other conditions involving a different level of marginal effective exposure.

Empirical establishment of equation (46) as a discovery criterion marks the end of the first stage of this analysis. The second stage will now be directed toward the development of an actual correction factor.

CORRECTION FACTOR FOR MASS AND VELOCITY BIAS

Equation (46) expressing the discovery criterion C_{marg} can be interrelated with the widely accepted relation between meteoroid mass and influx rate as expressed by equation (1) to provide a true correction factor for use as in equation (2). The correction factor can be derived readily with an assumption that the threshold level of exposure, as defined by the discovery criterion C_{marg} of equation (46), is sharply defined. A direct derivation under any other assumption would be more difficult. In appendix F, however, it is argued that if the correction factor is valid for a sharp threshold, it is then necessarily valid for diffuse thresholds also.

In development of the correcting factor, the dimensions of $F_{>m}$ and m in equation (1) are of no consequence, nor is the value of α . Although a degree of uncertainty exists regarding the value of α , a value of β equal to 1.34 from reference 4 is accepted widely.

Development of the correcting factor is based on an assumption that approximately the same velocity distribution and the same distribution of zenith angle exist for all masses within the photographic region and on the corollary assumption that approximately the same mass distribution exists for all velocities and for all zenith angles.

An infinite family of classes of meteors in two parameters is considered. Those classes are referred to as "velocity-zenith-angle" classes, and they are designated $C(v_\infty, Z_R)_i, C(v_\infty, Z_R)_j, C(v_\infty, Z_R)_k$. They consist of all specific combinations of velocity classes such as v_l, v_m, v_n and zenith-angle classes such as $Z_{R(o)}, Z_{R(p)}, Z_{R(q)}$. It should be understood that the classes of velocity or zenith angle may involve ranges of the pertinent parameter as small as necessary to avoid any question of indefiniteness in the treatment. Such ranges need not necessarily be of uniform size.

From the published data in reference 2, a set of values could be obtained for F_{i0}, F_{j0}, F_{k0} , where, for example, F_{i0} signifies an observed influx rate or an actual count of meteors within a velocity-zenith-angle class $C(v_\infty, Z_R)_i$. The values F_{i0}, F_{j0}, F_{k0} would include within each pertinent class all the meteors that produced at least sufficient photographic density to satisfy equation (46). The meteors so counted would include all masses that were actually observed within the pertinent classes, but these masses would extend to a different lower limit for some classes than for others.

The objective now is to derive from the values of F_{i0}, F_{j0}, F_{k0} rates $F_{>m(i)}, F_{>m(j)}, F_{>m(k)}$, where, for example, the symbol $F_{>m(i)}$ signifies a real influx rate for particles of mass greater than m and within the velocity-zenith-angle class $C(v_\infty, Z_R)_i$. Any value such as $F_{>m(i)}$ should include not only observed particles but all particles of mass greater than m that are not observed because their trails on the photographic plates are too faint. The mass m may be any mass specified but should

be identical for each of the values $F_{>m(i)}$, $F_{>m(j)}$, $F_{>m(k)}$. Absolute values of $F_{>m(i)}$, $F_{>m(j)}$, $F_{>m(k)}$ will not be sought, but a set of values bearing the proper proportions to each other is desired.

The assumption of a sharp threshold exposure level is invoked at this point, for any particular velocity-zenith-angle class, and equation (46) consequently applies exactly as a discovery criterion. That is, any particle providing a value of C_{marg} in equation (46) less than the threshold value will not be observed, and any particle providing a greater value will be observed. For convenience, equation (46) will be rewritten as

$$C_{\text{disc}} = m_{\infty}^{1.02} F(v_{\infty}, Z_R)^{2.93} \quad (47)$$

where C_{disc} is the assumed sharply defined discovery criterion and

$$F(v_{\infty}, Z_R) = (\cos Z_R)^{0.057} F(Z_R)_{\text{av}}^{-0.184} v_{\infty} \quad (48)$$

Now masses m_i , m_j , m_k will be defined as values of m_{∞} that satisfy equation (47) with use of values of v_{∞} and Z_R corresponding to the classes $C(v_{\infty}, Z_R)_i$, $C(v_{\infty}, Z_R)_j$, $C(v_{\infty}, Z_R)_k$. Accordingly, from equation (47),

$$m_i^{1.02} F(v_{\infty}, Z_R)_i^{2.93} = m_j^{1.02} F(v_{\infty}, Z_R)_j^{2.93} = m_k^{1.02} F(v_{\infty}, Z_R)_k^{2.93} \quad (49)$$

where, for example, $F(v_{\infty}, Z_R)_i$ is the value of the left-hand side of equation (48), which is obtained from the right-hand side of the same equation with use of the values of v_{∞} and Z_R corresponding to the velocity-zenith-angle class $C(v_{\infty}, Z_R)_i$.

The assumption of the same mass distribution for all velocity-zenith-angle classes permits rewriting equation (1) as

$$F_{>m(i)} = \alpha_i m^{-\beta} \quad (50a)$$

$$F_{>m(j)} = \alpha_j m^{-\beta} \quad (50b)$$

$$F_{>m(k)} = \alpha_k m^{-\beta} \quad (50c)$$

where α_i , α_j , α_k are unknown constants analogous to the constant α of equation (1), and a summation of which over all velocity-zenith-angle classes will equal α of equation (1). (In eq. (50a), for example, the symbol $F_{>m(i)}$ designates the influx rate of

particles of mass greater than m within velocity-zenith-angle class i , not the influx rate of particles of mass greater than m_i .)

Now, considering any two velocity-zenith-angle classes such as $C(v_\infty, Z_R)_i$ and $C(v_\infty, Z_R)_j$ from multiple equation (49),

$$\left(\frac{m_i}{m_j}\right)^{1.02} = \left[\frac{F(v_\infty, Z_R)_j}{F(v_\infty, Z_R)_i}\right]^{2.93} \quad (51)$$

or

$$\frac{m_i}{m_j} = \left[\frac{F(v_\infty, Z_R)_j}{F(v_\infty, Z_R)_i}\right]^{2.87} \quad (52)$$

As all meteors involving particles of mass greater than m_i , m_j , m_k are observed within the pertinent velocity-zenith-angle classes, equations (50) are applicable with use of observed influx rates F_{i0} , F_{j0} , F_{k0} on the left side and the pertinent masses m_i , m_j , m_k on the right side. Accordingly,

$$F_{i0} = \alpha_i m_i^{-\beta} \quad (53a)$$

$$F_{j0} = \alpha_j m_j^{-\beta} \quad (53b)$$

$$F_{k0} = \alpha_k m_k^{-\beta} \quad (53c)$$

From equations (1) and (50),

$$\alpha_i = \frac{F_{>m(i)}}{F_{>m}} \alpha \quad (54a)$$

$$\alpha_j = \frac{F_{>m(j)}}{F_{>m}} \alpha \quad (54b)$$

$$\alpha_k = \frac{F_{>m(k)}}{F_{>m}} \alpha \quad (54c)$$

From equations (53) and (54),

$$F_{io} = \frac{F_{>m(i)}}{F_{>m}} \alpha m_i^{-\beta} \quad (55a)$$

$$F_{jo} = \frac{F_{>m(j)}}{F_{>m}} \alpha m_j^{-\beta} \quad (55b)$$

$$F_{ko} = \frac{F_{>m(k)}}{F_{>m}} \alpha m_k^{-\beta} \quad (55c)$$

From equations (55),

$$\frac{F_{io}}{F_{jo}} = \frac{F_{>m(i)}}{F_{>m(j)}} \left(\frac{m_i}{m_j} \right)^{-\beta} \quad (56)$$

From equations (52) and (56),

$$\frac{F_{>m(i)}}{F_{>m(j)}} = \frac{F_{io}}{F_{jo}} \left[\frac{F(v_\infty, Z_R)_j}{F(v_\infty, Z_R)_i} \right]^{2.87\beta} \quad (57)$$

or

$$\frac{F_{>m(i)}}{F_{>m(j)}} = \frac{\frac{F_{io}}{\left[F(v_\infty, Z_R)_i \right]^{2.87\beta}}}{\frac{F_{jo}}{\left[F(v_\infty, Z_R)_j \right]^{2.87\beta}}} \quad (58)$$

Equation (58) defines the desired set of real influx rates relative to any mass m that may be specified, so far as the proportions that interrelate those rates are concerned. The right-hand side of this equation is free of any function of mass. It follows from equation (58) that a proper weighting factor for correction of observed counts, both for mass and velocity bias, is

$$\varphi_{\text{cor}} = \frac{1}{\left[F(v_{\infty}, Z_R) \right]^{2.87\beta}} \quad (59)$$

except as this function may be modified by later considerations. The actual count of meteors in any category should be corrected for both biasing effects, as far as its relation to other counts is concerned, if each meteor observed were counted, not as one meteor, but as φ_{cor} meteors. The factor defined by equation (59) still needs to be modified, however, to take into account the variation of area of field of view of the cameras with meteor altitude.

For the value of β equal to 1.34, equation (59) becomes

$$\varphi_{\text{cor}} = \frac{1}{\left[F(v_{\infty}, Z_R) \right]^{3.85}} \quad (60)$$

The exponent of the denominator in equation (60) involves the ratio of exponents of v_{∞} and m_{∞} in equation (46) multiplied by the absolute value of the exponent of m in equation (1). Obviously, therefore, an error in the ratio of exponents in equation (46) would amount to a substantially larger error in equation (60).

The development of equation (60), applicable for either a sharp or a diffuse exposure threshold (see appendix F), marks the completion of stage two of this analysis. In stage three, which now follows, it only remains to consider the effect of meteor altitude upon area of camera field of view.

EFFECT OF METEOR ALTITUDE ON PHOTOGRAPHED AREA

The value of φ_{cor} in equation (60) is a relative inverse probability. For example, let it be assumed that the part of Earth's atmosphere within the field of view of the cameras encounters a meteoroid that belongs within velocity-zenith-angle class i . Assume that the mass of such meteoroid is unknown, but greater than some fixed value m , and that nothing is known about the values of v_{∞} and $\cos Z_R$. Let p_i represent the probability that such meteoroid will produce a meteor that will be discovered on the

photographic plates. The probability p_i will, of course, vary with the fixed value m that is selected. It follows, then, that

$$F_{i0} = p_i F_{>m(i)} \quad (61)$$

or

$$\frac{F_{i0}}{F_{j0}} = \frac{p_i F_{>m(i)}}{p_j F_{>m(j)}} \quad (62)$$

or

$$\frac{F_{>m(i)}}{F_{>m(j)}} = \frac{\frac{F_{i0}}{p_i}}{\frac{F_{j0}}{p_j}} \quad (63)$$

Comparison of equations (58), (59), and (63) shows that

$$\varphi_{\text{cor}(i)} \propto \frac{1}{p_i} \quad (64)$$

This inverse probability is governed by the effective exposure and the subjective effect of velocity on ease of discovery of a meteor trail. A small correction might be applied because meteors are photographed over a larger area at greater altitudes. For this purpose, the relative inverse probability expressed by equation (60) may be multiplied by a factor inversely proportional to the effective area of the field of view of the cameras at the altitude of the meteor.

Such correction involves various uncertainties. For example, because of the facts that the fields of view of the two cameras are most nearly identical at only one altitude and that a meteor must be photographed by both cameras to be included in the data of reference 2, the variation of effective area of field of view with altitude is not simple to express analytically. Another example of uncertainties involved is the fact that, for analysis, a meteor trail must be entirely within the fields of view of both cameras. This fact amounts, essentially, to a reduction of the area of the field of view in a manner that is difficult to relate to meteor altitude. Nevertheless, a simplified estimate of the effect of altitude will be made. Validity of the result must be regarded as uncertain unless

confirmed by later work.

From equations (23) and (34), the height of a meteor at maximum effective exposure should be approximately

$$h_{m.e.} = k_8 \left(\frac{m_\infty^{1/3} \cos Z_R}{v_\infty^2} \right)^{-0.0627} \quad (65)$$

where

$$k_8 = \left(\frac{2.080 \rho_m^{2/3} \zeta}{\Delta HA} \right)^{-0.0627} k_3 \quad (66)$$

The unity exponent of $\cos Z_R$ within the brackets of equation (65) is theoretical only. For reasons discussed in appendix E, the unity exponent will be reduced by 75.7 percent, and equation (65) will be rewritten as

$$h_{m.e.} = k_8 \left[\frac{m_\infty^{1/3} (\cos Z_R)^{0.243}}{v_\infty^2} \right]^{-0.0627} \quad (67)$$

Accordingly, as the inverse of the area of the field of view varies inversely as the square of the altitude and only proportional values are of interest, the value of φ_{cor} should become, from equations (48), (60), and (67),

$$\varphi_{cor} = m_\infty^{0.0418} \cos Z_R^{-0.189} F(Z_R)_{av}^{0.708} v_\infty^{-4.10} \quad (68)$$

Equation (68) has the undesired feature that mass has been reintroduced, though with a very low exponent. The correction applied by mass to so small a power is minor. Hence, substitution of an average value for mass should be sufficiently accurate and will allow mass to be eliminated again.

From equation (46), the lower limit of mass for a given velocity-zenith-angle class is

$$m_{min} = (C_{marg})^{0.98} v_\infty^{-2.87} (\cos Z_R)^{-0.164} F(Z_R)_{av}^{0.529} \quad (69)$$

By differentiation of equation (1),

$$dF_{>m} = -\alpha\beta m^{-(\beta+1)} dm \quad (70)$$

The average mass of particles of mass greater than m_{\min} must be

$$m_{av} = \frac{- \int_{m=m_{\min}}^{m=\infty} m dF_{>m}}{- \int_{m=m_{\min}}^{m=\infty} dF_{>m}} \quad (71)$$

or, from equations (70) and (71),

$$m_{av} = \frac{\beta}{\beta - 1} m_{\min} \quad (72)$$

From equations (69) and (72), with the value of 1.34 for β ,

$$m_{av} = \frac{1.34}{0.34} (C_{\text{marg}})^{0.98} v_{\infty}^{-2.87} (\cos Z_R)^{-0.164} F(Z_R)_{av}^{0.529} \quad (73)$$

From equations (68) and (73),

$$\varphi_{cor} = \left[\frac{1.34}{0.34} (C_{\text{marg}})^{0.98} \right]^{0.0418} (\cos Z_R)^{-0.196} F(Z_R)_{av}^{0.730} v_{\infty}^{-4.22} \quad (74)$$

In the expression for m_{\min} in equation (69), the expression C_{marg} may be regarded as a constant having the specific value necessary for discovery of a meteor trail. As the factor φ_{cor} is desired only for obtaining relative corrected values of the actual counts upon which it will operate, the constants may be deleted, and equation (74), with a change of subscript for the correction factor, becomes

$$\varphi_w = (\cos Z_R)^{-0.196} F(Z_R)_{av}^{0.730} v_{\infty}^{-4.22} \quad (75)$$

The factor φ_w as expressed by equation (75) represents the final result of the third and last stage of this analysis. However, because of uncertainties mentioned earlier, the exponent of v_{∞} in equation (75) should be regarded as uncertain within the range from -3.85 to -4.22.

CONCLUDING REMARKS

The value of the weighting factor ϕ_w that has been developed herein involves a negative value of the exponent of the velocity relative to Earth's atmosphere v_∞ approximately twice that used heretofore. However, that value appears to be well supported both theoretically and empirically, at least for application to the meteor data published by McCrosky and Posen. The value of the exponent, within the range from -3.85 to -4.22, contains as a factor a value that was theoretically derived and which was empirically revised by about 3 percent.

The uncertainty within the range from -3.85 to -4.22 involves solely the question of the effect of altitude on area of the field of view. It is believed, if this uncertainty could be eliminated, the result should be accurate in regard to the exponent of v_∞ within 3 percent.

In the correction factor developed, the exponents of the cosine of the zenith angle $\cos Z_R$ and the function of field position $F(Z_R)_{av}$ are not based on such accurate agreement of theory and empirical results as is the exponent of v_∞ . These exponents may not be important, however, in practical application. A statistical effect would be expected, upon variation of these exponents, only if a systematic relation exists between zenith angle and other parameters that might be subjected to statistical study. For the 100 test meteors considered, sufficient variation of statistical effect existed to permit the finding of optimum exponents for $\cos Z_R$ and $F(Z_R)_{av}$. The ranges of hours of the night and days of the year involved in the photography of a large number of meteors, however, might be sufficient that statistical cancellation of the influence of zenith angle could be expected, at least in part. That is, in application of the correction factor that has been developed to a large number of meteors, it is possible that the values of the exponents of $\cos Z_R$ and $F(Z_R)_{av}$ could be equated to zero with small effect on the statistical result.

It might be argued that the graphical method used for obtaining the data that has been used herein by McCrosky and Posen is not sufficiently accurate to justify great confidence in the results. The exponent of v_∞ , however, is based on theory that is closely supported by the statistical analysis of many meteors. Considerably more confidence is justified in a statistical result obtained from many approximate reductions of meteor trails than would be justified in a result obtained in the reduction of only one or two trails by the same method. Moreover, a small degree of scatter of plotted points involved in this analysis is a good indication of the reproducibility of the methods used in the reduction of the data by McCrosky and Posen. This scatter does not appear to be great enough to cast doubt on the results obtained here. Also, the standard deviation in adjusted magnitudes for 100 test meteors, 0.369 magnitude, appears to be too small to cast doubt on the validity of the results.

A lower limit value of original mass of a particle m_{∞} should be expected to exist above which virtually all meteors would be discovered on the photographic plates, even if their atmospheric velocity v_{∞} were at the lowest practical value, equal to the velocity of escape from Earth. If the correction factor developed is valid, then the same velocity distribution should be obtained with such meteors without such factor as is obtained for all meteors collectively with the factor. This possibility could well be investigated in possible future work.

An approximately doubled exponent of v_{∞} in the correction factor as compared with weighting factors in current use calls for a substantial reduction of many current estimates of average velocities of meteoroids relative to the Earth's surface. Similar substantial changes will be required in estimates of statistical values of any parameters, orbital elements, for example, that are associated with values of v_{∞} and which, therefore, have been estimated with use of a weighting factor incorporating v_{∞}^{-2} .

Lewis Research Center,
National Aeronautics and Space Administration,
Cleveland, Ohio, March 3, 1967,
120-27-04-36-22.

APPENDIX A

SYMBOLS

A	shape factor, unknown for particular meteor but theoretically usable to adjust various equations for effect of meteoroid shape
C_{disc}	empirical discovery criterion for meteor
C_{marg}	theoretical or empirical criterion for marginal photographic exposure
E	photographic exposure, eq. (4)
E_{eff}	effective photographic exposure, equivalent to photographic exposure but corrected for effect of reciprocity failure to provide definite relation to photographic density
$E_{\text{eff(max)}}$	maximum effective exposure produced by meteor on photographic emulsion at any point in its trail
F_h	function interrelating distance of meteor from camera to height above ground level in terms of position of meteor within field of view of camera, for camera station A, eq. (C7)
$F_{>m}$	influx rate, or frequency of encounter, of meteoroids of mass greater than m
$F(Z_R)$	function interrelating photographic exposure to meteoroid velocity and height in terms of zenith angle of meteor and its position within field of view of camera, eq. (18)
$F(Z_R)_{\text{av}}$	weighted average value of $F(Z_R)$ for all positions within field of view of cameras
$F(Z_R)_{\text{min}}$	minimum value of $F(Z_R)$ for all positions within field of view of cameras
$F_v(Z_R)$	function interrelating velocity of image on photographic emulsion to velocity of meteor particle relative to atmosphere in terms of zenith angle of meteor and its position within field of view of camera, eq. (C6) for camera station A
H	scale height for Earth's atmosphere or difference in altitude corresponding to air density ratio of e^{-1} , km
H_B	height of meteor above ground level at beginning of trail (ref. 2), km
h	altitude relative to sea level, km
h_g	height of meteor above ground level, km

$h_{m.e.}$	height of meteor above ground level at time of maximum effective exposure on photographic emulsion, km
I_i	image brightness in terms of luminous flux impinging on unit area of photographic plate
I_m	luminous intensity of meteor in terms of total luminous flux emanating from it
k_1	constant for conversion from proportionality (16) to eq. (17)
k_2	constant, eq. (21)
k_3	constant of proportionality, eq. (23)
k_4	constant, eq. (25)
k_5	constant, eq. (38)
k_8	constant, eq. (66)
M_{adj}	adjusted photographic magnitude of meteor, eq. (42)
M_{pg}	photographic magnitude of meteor (ref. 2)
m	instantaneous mass of meteoroid during ablation
$m_{m.e.}$	remaining mass of meteoroid when maximum effective exposure is produced on photographic emulsion
m_∞	original mass of meteoroid before ablation
n	number of shutter breaks within photograph of meteor trail (ref. 2)
T	duration of exposure of image on particular part of photographic emulsion
$V_{\mu, \nu, \xi}$	variance, eq. (44)
v	instantaneous velocity of meteor relative to atmosphere during process of ablation
v_i	instantaneous velocity of meteor image on photographic emulsion
v_∞	velocity of meteoroid relative to Earth's atmosphere before deceleration caused by atmosphere
Z_R	angle between meteor path in atmosphere and zenith
α	constant coefficient indicating frequency of encounter of meteoroids, eq. (1)
β	constant, negative value governs relation of frequency of encounter of meteoroids to lower limit of mass, eq. (1)
ζ	energy required to ablate one unit mass from meteoroid
Λ	efficiency of utilization of kinetic energy in ablation of mass of meteoroid

μ	tentative exponent of v_{∞} in expression for discovery criterion for meteor
ν	tentative exponent of $\cos Z_R$ in expression for discovery criterion of meteor
ξ	tentative negative exponent of $F(Z_R)$ in expression for discovery criterion for meteor
ρ	density of Earth's atmosphere at particular altitude
ρ_m	density of meteoroid
$\rho_{m.e.}$	density of Earth's atmosphere at altitude of meteoroid when maximum effective exposure is produced on photographic emulsion
τ	luminous efficiency of meteor, approximately fraction of lost kinetic energy of meteoroid that is converted to photographable radiation
φ_{cor}	tentative correction factor by which actual count of meteors in various categories of v_{∞} and Z_R may be multiplied to produce correct ratios of counts in all categories, on basis of same lower mass limit for all categories
φ_w	final value of φ_{cor} , eq. (75)

APPENDIX B

APPROXIMATE RELATION OF AIR DENSITY TO ALTITUDE

Analytical simplification can be effected by an approximation in which a power relation is used over a limited range for the dependency of atmospheric density upon altitude above sea level. The well known more accurate relation is shown by equation (22). As a first step in estimating the power relation, determination of a practical range of altitudes for photographic meteors was necessary.

Estimation of a Practical Range of Altitude for Photographic Meteors

A computer scan of the data for 2039 sporadic meteors showed that meteor 8047 started at the greatest altitude, 132.3 kilometers, and that meteor 7946 reached the lowest altitude, 46.0 kilometers (ref. 2, p. 59, lines 38 and 19, respectively). In the scanning procedure, the minimum altitude for each meteor was calculated as $h_{m.e.}$ of equation (41). Meteors for which no mass was determined were excluded from consideration. According to the same computer scan, meteor 4330 was 51st in descending order of starting altitude at 115.9 kilometers (ref. 2, p. 66, line 18). Meteor 7210 was 51st in order of ascending minimum altitudes reached at 71.2 kilometers (ref. 2, p. 46, line 18). Hence, the altitudes of 115.9 and 71.2 kilometers represent the $2\frac{1}{2}$ -percent points at each end of the range of altitudes.

By standard statistical practice, regions beyond the $2\frac{1}{2}$ -percent points can often be ignored. But, before either of these ranges can be rejected as including only a negligible fraction of the total number of meteors, the possibility must be considered that such fraction of the total possesses some characteristic of special importance. The highest starting altitudes for meteor trails might be expected to be characteristic of meteor particles of highest speeds and substantial mass. Also, the lowest range of altitudes might be expected to be reached principally by relatively slow meteor particles of large initial mass.

The actual unimportance of the $2\frac{1}{2}$ -percent regions is demonstrated in figure 5. Starting and ending altitudes are shown for each of 100 test meteors in the order in which they are listed in table I. Although the figure verifies the expected relation of meteor speed to starting and ending altitude, only three test meteors appear within the $2\frac{1}{2}$ -percent regions, and they do so by only small margins. This analysis is concerned primarily with marginal brightness of meteors, which is the standard by which the 100 test meteors were chosen. Hence, substantially brighter meteors falling within the $2\frac{1}{2}$ -percent regions are not important here. It might be argued that the aerodynamic

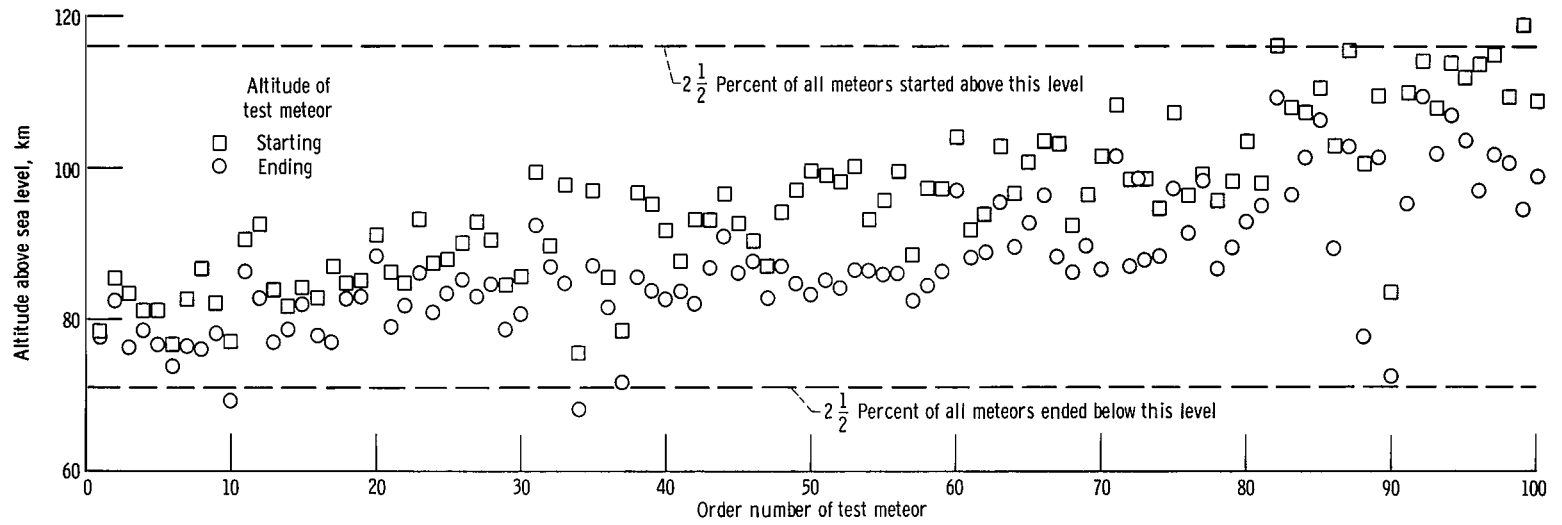


Figure 5. - Altitudes of test meteors.

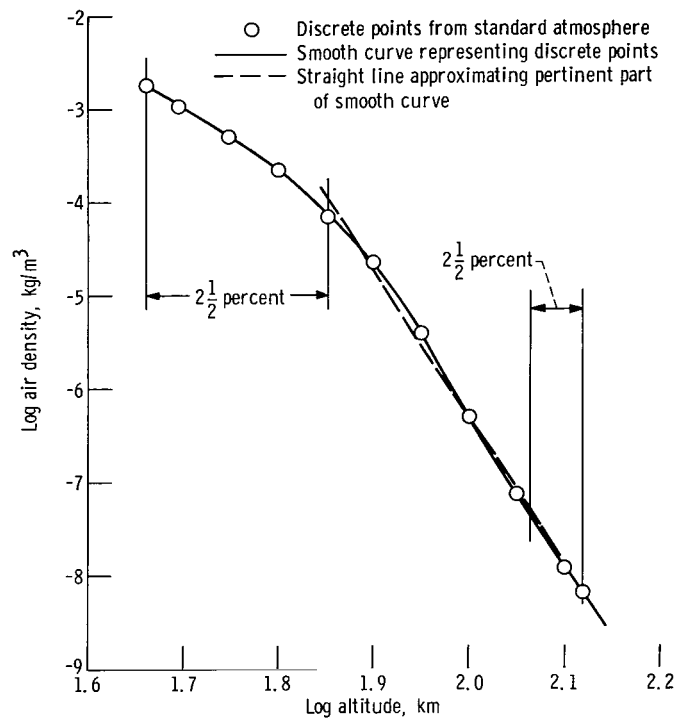


Figure 6. - Variation of air density with altitude.

history of a meteor even before it becomes visible could be important. Figure 6, however, shows that a straight line well represents the actual curve throughout the upper $2\frac{1}{2}$ -percent region and probably some distance beyond at the high-altitude end.

On the basis of these considerations, an altitude range from 71 to 116 kilometers appears to be within practical limits for the meteors reported in reference 2.

Deduction of Approximate Expression for Air Density in Relation to Altitude

Figure 6 shows the relation of air density to altitude on a log-log plot for the entire range of altitudes covered by the sporadic meteors reported in reference 2. The discrete points used in the figure for construction of the curve were obtained from the U.S. Standard Atmosphere, 1962 (ref. 10). The dashed line in figure 6 was drawn according to visual estimate as the best straight line to represent the curve of plotted data in the region between the $2\frac{1}{2}$ -percent points. The slope of that line, with due allowance for the great difference in scales of ordinates and abscissas, is $-1/0.0627$. Hence, the straight line represents the power relation expressed by equation (23).

Among the 100 test meteors, the greatest error in the straight-line relation shown in figure 6 would apply to the single meteor that reached an altitude of 68 kilometers, meteor 6889 (ref. 2, p. 41, line 46). For that altitude, the data curve of figure 6 indicates a log density of approximately -3.97 . The straight line indicates a log density of about -3.67 . The difference between these two logarithmic values amounts to an overestimate of air density by a factor of about 2.0. From the manner of derivation of equation (39), this meteor would seem to be treated as producing maximum effective exposure at only slightly too high an altitude and also at a value of remaining mass slightly too high. Its actual effective exposure should be approximately twice that given by equation (39). This factor amounts to an excess calculated magnitude of 0.75, only about 30 percent greater than the standard deviation in magnitude for all the test meteors as discussed in the section, Appraisal of Revised Criterion for Discovery of Image Trail.

The inaccuracy of the straight line in figure 6, even for the worst case, appears to be within reasonable limits. Hence, equation (23) should be sufficiently accurate for its purpose.

APPENDIX C

STATISTICAL EFFECT OF POSITION OF METEOR WITHIN FIELD OF VIEW OF CAMERAS

Information is not readily available regarding the location of a meteor trail within the field of view of the cameras used in obtaining the data for reference 2. Hence, considerable uncertainty exists regarding the relation of image velocity on the photographic emulsions to actual velocity of the meteor particle and regarding the relation of meteor distance from cameras to meteor altitude. Both these relations enter into any estimation of effective exposure on the photographic plate. It was consequently necessary, in conjunction with this analysis, to develop a minimum function and a statistical average function to compensate as well as possible for the lack of information concerning field positions of meteors. Such functions were computed individually for each meteor.

The problem has been treated as reported here with the objective of determining and combining two functions: (1) $F_v(Z_R)$, a function for various parts of the field of view involving meteor particle velocity relative to the atmosphere v_∞ , the zenith angle Z_R , the azimuth of the meteor path, and the velocity of the image v_i and (2) F_h , a function for those same parts of the field of view involving meteor height, zenith angle, azimuth of meteor path, and distance between meteor particle and camera.

Proportionality (6) correctly interrelates the image speeds v_i for different meteors if $F_v(Z_R)$ and F_h are arbitrarily equated to unity, if each meteor is located directly above the cameras, and if each meteor has a zenith angle of 90° . As the expression is a proportionality rather than an equation, $F_v(Z_R)$, for a particular height above ground level, a particular field position, a particular value of zenith angle, and a particular azimuth, may be defined as ratio of image velocity v_i to the velocity of the meteor particle relative to the atmosphere v_∞ . Also, from the discussion immediately preceding equation (5), F_h for the same group of parameters is the ratio of distance between meteor particle and camera to the altitude above ground level.

The combination of the two functions $F_v(Z_R)$ and F_h , according to equation (E1), was designed to express as $F(Z_R)$ a dependency of image exposure upon particle velocity, particle height, cosine of the zenith angle, and azimuth of the meteor path for many parts of the field of view. From the many values of $F(Z_R)$, a minimum was chosen and designated $F(Z_R)_{\min}$. Also, a weighted average was calculated and designated $F(Z_R)_{\text{av}}$.

All data needed for calculation of $F(Z_R)_{\min}$ and $F(Z_R)_{\text{av}}$ are given in reference 2 for each meteor except azimuth of the meteor path. The azimuth, however, can be computed for each meteor from the data given in reference 2 on (1) right ascension of

true radiant, (2) declination of true radiant, (3) geocentric velocity of meteoroid before acceleration by Earth's gravity, (4) velocity of meteoroid relative to atmosphere v_{∞} , (5) zenith angle, (6) latitude and longitude of camera locations, and (7) exact day and hour of impact. It is not believed justifiable to use space here to describe the method of computing the azimuth because an explanation would be involved and lengthy and because the method could be generated quickly by anyone accustomed to working with gravitational trajectories, with an assumption of free fall of the meteoroid within a plane containing the meteor path and the center of the Earth.

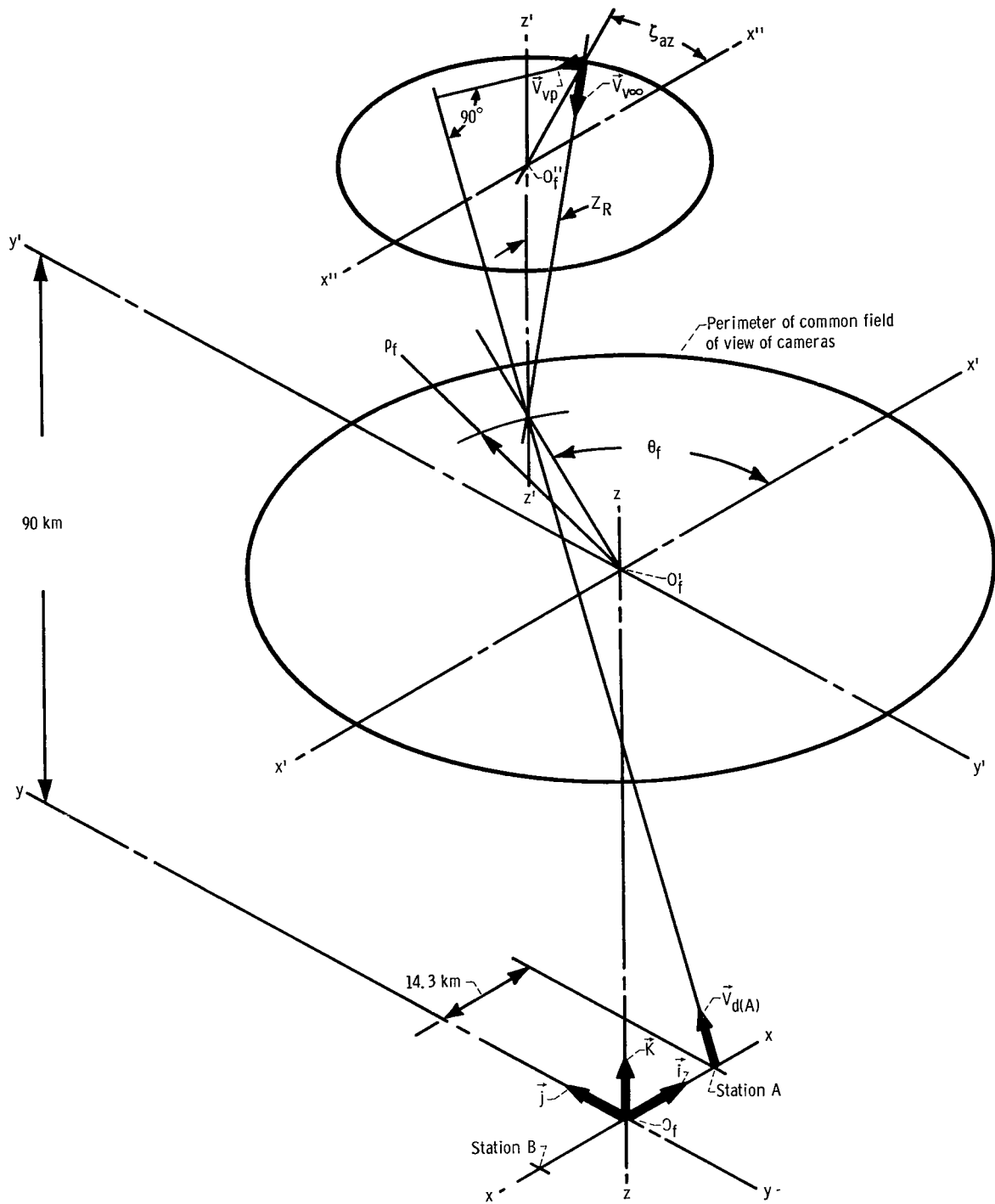
For each part of the field of view considered, values of $F(Z_R)$ were determined for each of the two camera stations and were designated $F(Z_R)_A$ and $F(Z_R)_B$. A manner of choice between the two values will be described later.

Method of Determining Relation Between Velocity of Image and Velocity of Meteor

With all other things equal, image velocity on the photographic plate is always proportional to meteor particle velocity. Hence, the problem of determining the parameter $F_v(Z_R)$ for a particular position within the field of view was essentially that of determining the ratio of path lengths of image and meteor particle for a very short path. The method used will be described with vector notations.

A local set of coordinates x, y, z was established with origin O_f at the midpoint of a line on Earth's surface interconnecting camera stations A and B, which were at locations of longitude and latitude stated by Hawkins (ref. 15). The positive direction of the x -axis was taken as extending from the origin horizontally toward the geographical location of camera station A. The positive direction of the y -axis was taken horizontally, 90° counterclockwise from the positive direction of the x -axis, and the positive direction of the z -axis was taken as straight upward. Three unit vectors $\vec{i}, \vec{j},$ and \vec{k} were defined as extending in the positive directions of the $x, y,$ and z axes.

The coordinate axes, the camera stations, the unit vectors, and other entities that were used are illustrated in the following sketch. The distance 14.3 kilometers shown in the sketch was taken from reference 2. For simplicity and because no great statistical error should result, the altitude of 90 kilometers shown in the sketch was taken as the approximate midpoint of the practical range of meteor altitudes as found in appendix B. For the purpose of definition of a particular field position, the origin O'_f was taken at an altitude of 90 kilometers directly above origin O_f , and axes $x' - x'$ and $y' - y'$ were constructed through the origin O'_f parallel to the axes $x - x$ and $y - y$. The field position was then defined as being located at angle θ_f measured counterclock-



wise from the positive direction of axis $x' - x'$ and at a distance ρ_f from the origin O'_f . A particular meteor under consideration was assumed to reach the field position so defined. For the purpose of defining the direction of its path, an axis $z' - z'$ was constructed through the field position parallel to axis $z - z$. At an unspecified height above the field position an axis $x'' - x''$ was constructed through axis $z' - z'$ and parallel to axes $x - x$ and $x' - x'$. The azimuth of the meteor path was then defined by the angle ζ_{az} . That angle was measured within a horizontal plane, in the counterclockwise direction, from the positive direction of axis $x'' - x''$ to the common plane of the meteor path and the axis $z' - z'$. The angle between the meteor path and the axis $z' - z'$, that is the angle Z_R , then completed the specification of the meteor path.

A unit length of the meteor path was then represented by the unit vector \vec{V}_{v_∞} , expressed by the equation

$$\vec{V}_{v_\infty} = -\sin Z_R \cos \zeta_{az} \vec{i} - \sin Z_R \sin \zeta_{az} \vec{j} - \cos Z_R \vec{k} \quad (C1)$$

Next, for station A, a unit vector $\vec{V}_{d(A)}$ was constructed from station A in the direction toward the field location in question. This vector was expressed by the equation

$$\vec{V}_{d(A)} = \frac{(-14.3 + \rho_f \cos \theta_f) \vec{i} + \rho_f \sin \theta_f \vec{j} + 90 \vec{k}}{\sqrt{(\rho_f \cos \theta_f - 14.3)^2 + (\rho_f \sin \theta_f)^2 + 90^2}} \quad (C2)$$

(For station B, the equation was the same except that the sign was positive for the distance 14.3 km.)

The vector \vec{V}_{vp} , component of \vec{V}_{v_∞} perpendicular to $\vec{V}_{d(A)}$, was determined by the equation

$$\vec{V}_{vp} = \vec{V}_{v_\infty} - \left(\vec{V}_{v_\infty} \cdot \vec{V}_{d(A)} \right) \vec{V}_{d(A)} \quad (C3)$$

The scalar distance $l_{f(A)}$ from station A to the field position was

$$l_{f(A)} = \sqrt{(\rho_f \cos \theta_f - 14.3)^2 + (\rho_f \sin \theta_f)^2 + 90^2} \quad (C4)$$

The distance of image movement on plate in the cameras \vec{V}_{vp} used for the photographs of reference 2 is closely proportional to the numerical value of \vec{V}_{vp} divided by the distance from meteor particle to camera. As only relative values of image velocity on the photographic plate are of interest, the distance of image movement was therefore taken as

$$d_i = \frac{|\vec{V}_{vp}|}{l_{f(A)}} \quad (C5)$$

As a unit vector was used for $\vec{V}_{v\infty}$, the value of d_i in equation (C5) represents the ratio of the distance of movement of image to the distance of movement of the meteor particle, as well as the ratio of velocities. Hence, the desired parameter $F_v(Z_R)_A$ is equal to d_i , or

$$F_v(Z_R)_A = \frac{|\vec{V}_{vp}|}{l_{f(A)}} \quad (C6)$$

The value of $F_v(Z_R)_B$ was determined in an analogous manner.

Method of Determining Relation Between Meteor Distance and Altitude Above Ground Level

From the discussion in the preceding section, for a given field position, the ratio of distance between meteor and camera to height above ground level is obviously equal to $l_{f(A)}$ as given by equation (C4) (for station A) divided by the meteor height. That is, for station A,

$$F_h(A) = \frac{\sqrt{(\rho_f \cos \theta_f - 14.3)^2 + (\rho_f \sin \theta_f)^2 + 90^2}}{90} \quad (C7)$$

(For station B, the sign is positive for the distance 14.3 km.)

Combined Function of Image Speed and Camera Distance

In accordance with equation (E1), two values of $F(Z_R)$ were determined for each field position considered, for stations A and B. Those two values were

$$F(Z_R)_A = F_h(A) F_v(Z_R)_A \quad (C8)$$

and

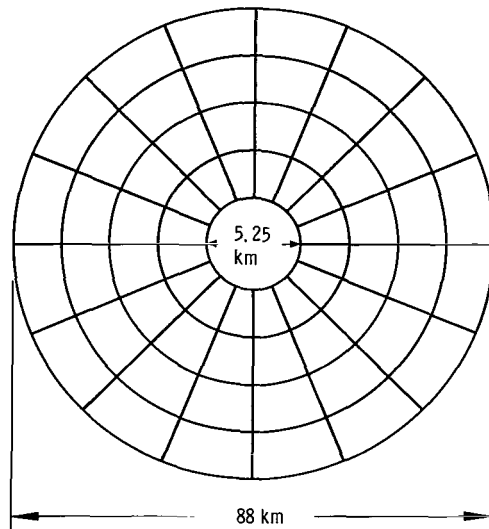
$$F(Z_R)_B = F_{h(B)} F_v(Z_R)_B \quad (C9)$$

In general, the values of $F(Z_R)_A$ and $F(Z_R)_B$ were appreciably different. As the analysis described in the main text was concerned with marginal exposure densities, the value $F(Z_R)_A$ or $F(Z_R)_B$ that would produce the fainter exposure is the value of controlling importance.

In the work reported in reference 2, the meteor path on one photographic plate had to be visible through the other plate. Such a requirement does not appear to alter the conclusion that the fainter trace should control. For, in the viewing of a trace through two plates rather than one, the increased background absorption and scatter of light is the same whether the trace that must be seen is on the upper or the lower plate. In other words, the increased difficulty in seeing a trace by light transmitted through two plates in contact should be substantially the same, whether the trace is on one plate or the other. From the discussions and equations in the main text, it is apparent that the fainter photographic trace occurs with the greater value of $F(Z_R)$. Accordingly, for each field position considered, the higher value, $F(Z_R)_A$ or $F(Z_R)_B$, was chosen and used as $F(Z_R)$.

Minimum and Statistical Average Values for Combined Function

For determination of minimum and statistical average values of the combined function, $F(Z_R)_{\min}$ and $F(Z_R)_{\text{av}}$, the common field of view of the cameras was divided into $4n_f^2$ zones bounded by concentric circles and radial lines, where n_f is a variable to which a series of values was given during the entire course of the determinations. The manner of division of the field of view, with n_f equal to 4, is illustrated in the following sketch.



The external diameter of 88 kilometers represents the outer limit of the camera field of view. The internal diameter of 5.25 kilometers represents an unphotographed area caused by the shaft and the hub of a rotating shutter mounted within each camera. The cameras with which the photographs were exposed have been described in various publications (refs. 16 to 18). The external diameter of the field of view at an altitude of 90 kilometers was deduced from the total effective field angle of 55° and the statement in reference 2 that the rotating shutter did not cover the outer 12 percent of the field of view. The diameter of 5.25 kilometers for the blind area in the center of the field of view was obtained by scaling the diameter of the internal spot devoid of star images relative to the external diameter from plate 2 of reference 13. The spacing between the $(n_f + 1)$ circles and the $4n_f^2$ radial lines was uniform.

For each of the $4n_f^2$ zones, a value of ρ_f and a value of θ_f were used corresponding to the exact center of the zone, for determinations of values of $F(Z_R)$ in the manner previously described. The smallest such result obtained for any of the $4n_f^2$ zones was recorded as $F(Z_R)_{\min}$. For the determination of $F(Z_R)_{\text{av}}$, the following steps were performed:

(1) For each of the $4n_f^2$ zones, an area factor was taken equal to ρ_f .

(2) For each of the $4n_f^2$ zones, a probability factor p_f was determined in a manner that will now be described. With all else equal, the discussions in the section Express-

sion for Maximum Effective Exposure (eq. (39)) show that the exposure should be nearly inversely proportional to $F(Z_R)$ and directly proportional to m_∞ . Hence, with the definite values of v_∞ and $\cos Z_R$ known for the meteor, for marginal photographic density the value of m_∞ should be approximately proportional to $F(Z_R)$. From equation (1), with $\beta = 1.34$, the frequency of occurrence of meteors of mass greater than the marginal value should therefore be governed by the proportionality

$$p_f \propto F(Z_R)^{-1.34} \quad (C10)$$

or, as only relative values are of interest,

$$p_f = F(Z_R)^{-1.34} \quad (C11)$$

(3) The value of $F(Z_R)_{av}$ was determined from the equation

$$F(Z_R)_{av} = \frac{\sum_{i=1}^{i=4n_f^2} F(Z_R)_{(i)}^{\rho_{f(i)}} p_{f(i)}}{\sum_{i=1}^{i=4n_f^2} \rho_{f(i)} p_{f(i)}} \quad (C12)$$

The area factor ρ_f becomes increasingly exact with increasing values of n_f , and the value of $F(Z_R)_{av}$ becomes more exact also because the computation for each zone is more uniformly representative of the entire zone. The procedure that has been described was performed for each meteor with values of n_f equal to 4 and to 7. As the computer time increased at a prohibitive rate beyond $n_f = 7$ and as the difference in results between the values of 4 and 7 was insignificant, no determination was made with a greater value of n_f .

APPENDIX D

EFFECT OF METEOROID FRAGMENTATION

In the main text a criterion for marginal photographic exposure of a meteor trail, equation (40), is derived theoretically without taking into account the so-called faint-meteor anomaly, convincingly ascribed by Jacchia (ref. 14) to meteoroid fragmentation. Because of the complexity of the subject of fragmentation and because of insufficient knowledge concerning it, derivation of an analogous equation including the effects of fragmentation would not be possible at this time. To a certain extent, however, equation (40) should apply to the fragments of a meteoroid individually.

Consider for example two extreme cases, mutually independent, in which (1) a meteor breaks into 10 fragments of equal mass infinitely early in its encounter with Earth's atmosphere and (2) a meteor breaks into 10 fragments of equal mass at the instant when $E_{\text{eff(max)}}$ is reached in accordance with equation (39). In case (1), equation (39) applies to each of the 10 fragments, but with use of one-tenth the original value of m_{∞} . Also, the value of $E_{\text{eff(max)}}$ given by equation (39) should be multiplied by the number of particles. The result indicates approximately a 4.5-percent decrease in value of $E_{\text{eff(max)}}$ of equation (39) or a 4.5-percent error involved in the application of C_{marg} from equation (40). If the exponent of m_{∞} were taken as unity instead of 1.02, no change in value of $E_{\text{eff(max)}}$ should occur, and hence no error should exist in the application of C_{marg} from equation (40).

In case (2) an assumption may be made, the validity of which will be shown later, that although the 10 fragments increase their exposure level at the time of fragmentation, they do not do so after that time. In that case, the ratio of values of $R_{\text{eff(max)}}$ for the fragmented and unfragmented condition should be the same as the ratio of values of I_m as given by equation (19). Such ratio would be the cube root of the number of fragments. That is, the value of $E_{\text{eff(max)}}$ should increase by a factor of about 2.15. If the meteoroid had broken into only two fragments, the factor would be only 1.26.

That the 10 fragments do not increase their exposure levels at a later time than the time of fragmentation, in case (2), is shown as follows: At the instant of fragmentation the same condition develops as if the 10 fragments were actually 10 meteoroids that had arrived earlier at the outer limit of Earth's atmosphere, each having an original mass that may be designated $m_{\infty <}$ and all traveling too near each other to be resolved by the cameras but far enough apart that the individual aerodynamic effects would be independent. Such an equivalent condition would be essentially similar to the real condition of case (1). The remaining mass of each of the 10 hypothetical meteoroids, at the time corresponding to fragmentation, would be one-tenth the remaining mass of the unfragmented meteoroid at the time of fragmentation, under the real condition of case (2). Obviously $m_{\infty <}$ would

be less than m_{∞} , the original mass of the unfragmented meteoroid of case (2).

Consequently, for the hypothetical 10 meteoroids the value of $\rho_{m.e.}$ from equation (34) obtained by substituting $m_{\infty <}$ for m_{∞} would be less than for the unfragmented meteoroid with use of m_{∞} . This fact means that the 10 hypothetical meteoroids of the assumed equivalent condition would have passed their position of maximum effective exposure before the time of fragmentation of the real meteoroid. Hence, the fragmented meteoroid would reach its maximum effective exposure at the instant of fragmentation, not later, and the indication from equation (19) of increase in value of $E_{\text{eff(max)}}$ by a factor of about 2.15 should be valid.

The increase of $E_{\text{eff(max)}}$ by a factor of 2.15 amounts to a decrease of 0.83 magnitude. The factor 1.26 corresponds to 0.25 decrease in magnitude. Application of C_{marg} from equation (40) involves errors of the same magnitudes.

It is seen that the effect of fragmentation is to multiply the value of $E_{\text{eff(max)}}$ from equation (39) by a random factor, which depends on the altitude at which fragmentation occurs and on the number of particles formed. Although the shape factors of the particles have been ignored, their effect should not be significant statistically. The likely values of the random multiplying factor do not appear to be great enough to destroy the statistical value of the criterion C_{marg} of equation (40).

APPENDIX E

MISCELLANEOUS EFFECTS INVOLVING POSITION OF METEOR WITHIN FIELD OF VIEW

Statistical Effect of Position of Meteor Within Field of View

Values of $F(Z_R)_{\min}$ and $F(Z_R)_{\text{av}}$ for each of the meteors reported in reference 2 were determined by a statistical method explained in appendix C. The function $F(Z_R)_{\min}$ was intended only for use in the comparison of values of C_{marg} (eq. (43)) for the 100 test meteors described in the text and in table I. The function $F(Z_R)_{\text{av}}$ was intended for use in later statistical studies. The function $F(Z_R)_{\text{av}}$ as described in appendix C was designed to give the best statistically expected value that could be determined from the data available in reference 2 to the effective exposure E_{eff} according to equation (17). The function $F(Z_R)_{\min}$ was designed to give to the effective exposure E_{eff} according to equation (17) the maximum value that it could have for any position of the meteor within the camera field of view.

The values of $F(Z_R)_{\min}$ and $F(Z_R)_{\text{av}}$ (shown for the 100 test meteors in table I) were computed according to the equation

$$F(Z_R) = F_h F_v(Z_R) \quad (\text{E1})$$

After much use had been made of these values, it was discovered that $F(Z_R)$ should be defined by equation (18). Uncertainties involved in the computation and the use of the function $F(Z_R)$ are believed to be too great to justify repetition of the effort that was expended in the computation and use of these values. Hence, the values of these functions in table I and the values that have been computed and recorded for 2039 sporadic meteors of reference 2 are in accordance with equation (E1) rather than equation (18).

Relation of Meteor Position Within Camera Field of View to Selection of Test Meteors

In the selection of the 100 test meteors, it was desirable that each such meteor should occupy a position within the field of view for which the statistically expected value

of E_{eff} according to equation (17) would exist. If such condition had been possible, use of equation (43) with $F(Z_R)_{\text{av}}$ for $F(Z_R)$ would have led directly to determination of the best exponent for $F(Z_R)_{\text{av}}$ in that equation.

But no method was discovered for selection of test meteors that would consistently involve an average position within the camera field of view, such as would give E_{eff} its statistically expected value. Hence, there could be no confidence that use of $F(Z_R)_{\text{av}}$ in equation (43) would necessarily lead to the best exponent ξ for $F(Z_R)_{\text{av}}$ in that equation.

Actually, for the method of selection used, it was to be expected that the test meteor chosen within a subclass should occupy one of the more favorable field positions from the standpoint of producing a large value of E_{eff} . That is, it was to be expected that the function $F(Z_R)_{\text{min}}$ should apply in equation (43). It was suspected, however, and results confirmed, that approximately equivalent results would be obtained whether use was made of $F(Z_R)_{\text{min}}$ or $F(Z_R)_{\text{av}}$. The expectation that the test meteors should occupy the more favorable positions within the camera field of view is based on the following reasoning.

Among all meteors within a given subclass, various positions within the camera field of view were involved. For a given value of M_{adj} in step (4) of the selection procedure, the different field positions provided different effective exposures because of different distances of meteor from camera and different image velocities on the plates. Hence, some field positions were more favorable than others from the standpoint of discovery of a meteor trail. But, if the meteors within a subclass are sufficiently numerous and if from among them that meteor is chosen which had the first or second greatest photographic magnitude as reported in reference 2, that meteor should have occupied one of the more favorable locations. Such a conclusion seems justified because the authors of reference 2 were able to use the meteor location relative to the cameras in their determination of photographic magnitude, and presumably they did so. In any large sample, within narrow ranges of velocity and zenith angle, a meteor should be found in a favorable location having greater magnitude than could have been detected in less favorable locations. The sample need not be very large because of the well known fact that meteors having large positive values of magnitude are much more numerous than those having smaller magnitudes.

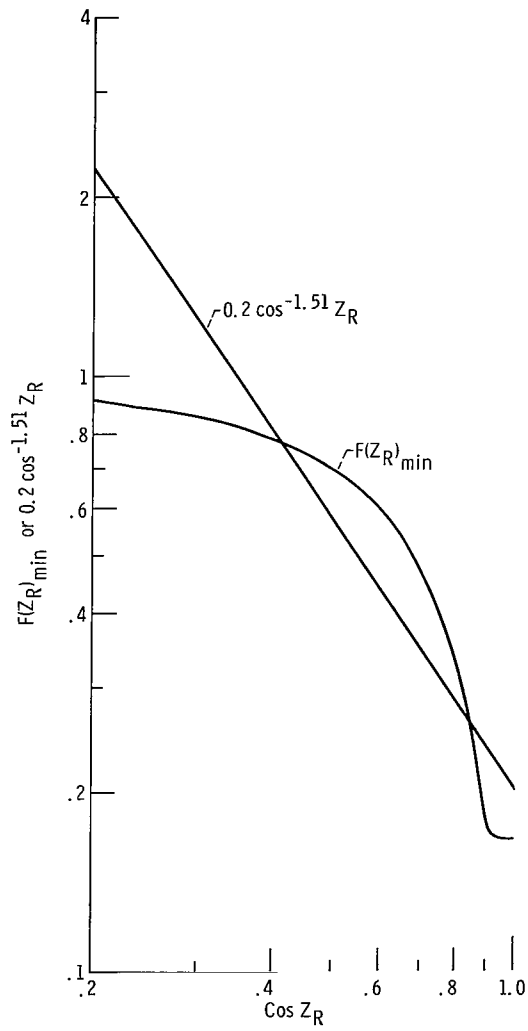


Figure 7. - Variation of statistical function $F(Z_R)_{\min}$ with $\cos Z_R$, where Z_R is zenith angle.

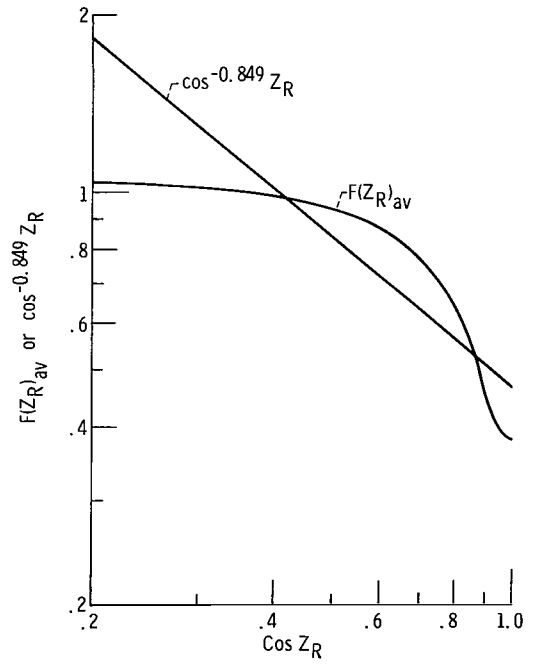


Figure 8. - Variation of statistical function $F(Z_R)_{\text{av}}$ with $\cos Z_R$, where Z_R is zenith angle.

Relation of Function of Meteor Position Within Camera Field of View to Expression for Marginal Photographic Exposure

As stated in discussion of equation (45), the function $F(Z_R)_{\min}$ contains implicitly a factor equal to a negative power of $\cos Z_R$. The same is true of the function $F(Z_R)_{\text{av}}$. These facts must be considered in a complete appraisal of equation (45) as a criterion for marginal exposure density from the standpoint of discovery of a meteor trail.

When values of $F(Z_R)_{\min}$ and $F(Z_R)_{\text{av}}$ were computed according to the method described in appendix C for 2039 sporadic meteors, mean values of those functions were also computed for each value of $\cos Z_R$ in increments of 0.01. Figure 7 shows such mean values of $F(Z_R)_{\min}$ in relation to values of $\cos Z_R$ on a log-log scale. Also shown in figure 7 as a straight line is a representation of the function $(0.2 \cos^{-1.51} Z_R)$. Such function was found by the method of least squares to be the best representation of $F(Z_R)_{\min}$ as a straight line in figure 7, with weighting of the various values of $\cos Z_R$ according to their frequencies of occurrence among the 100 test meteors. As the 100 test meteors tended toward higher values of $\cos Z_R$, the straight line in figure 7 tends to conform better with the right-hand part of the curve representing $F(Z_R)_{\min}$.

The straight-line relation shown in figure 7 will not be used here as a substitute for $F(Z_R)_{\min}$. However, as only relative values of $F(Z_R)$ are of interest, $F(Z_R)_{\min}$ may be represented approximately as

$$F(Z_R)_{\min} = (\cos Z_R)^{-1.51} F'(Z_R)_{\min} \quad (\text{E2})$$

where $F'(Z_R)_{\min}$ may be defined as that portion of $F(Z_R)_{\min}$ which does not contain any positive or negative power of $\cos Z_R$ as a factor.

Hence, equation (45) may be rewritten as

$$C_{\text{marg}} = m_{\infty}^{1.020} v_{\infty}^{2.93} (\cos Z_R)^{0.625} F'(Z_R)_{\min}^{-0.54} \quad (\text{E3})$$

Thus, the result, rather than a complete repudiation of the theoretically derived factor $(\cos Z_R)^{1.060}$ in equation (40), is really a 75.7-percent reduction of the combined exponent of $\cos Z_R$ in its own right and $\cos Z_R$ as contained implicitly within the factor $F(Z_R)_{\min}^{-1}$. For, equation (40) may be rewritten as

$$C_{\text{marg}} = m_{\infty}^{1.020} v_{\infty}^{2.842} (\cos Z_R)^{2.57} F'(Z_R)^{-1} \quad (\text{E4})$$

and the exponent of $\cos Z_R$ in equation (E3) is 75.7 percent lower than in equation (E4). At the same time, an approximate 50-percent reduction is applied to the exponent of $F'(Z_R)$. Nothing can be concluded as to the portion of the reduction of exponent that should be applied directly to the $(\cos Z_R)^{1.060}$ factor and the portion that should be applied to the negative power of $\cos Z_R$ contained within the function $F(Z_R)_{\text{min}}$. For lack of evidence for a better procedure, where necessary the 75.7-percent reduction is assumed to apply equally to the exponent of $\cos Z_R$ in its own right and to the implicit $(\cos Z_R)^{-1.51}$ contained within the function $F(Z_R)_{\text{min}}$.

The large empirical change in the exponent of $F'(Z_R)_{\text{min}}$ is not disturbing. The method of computing the functions $F(Z_R)_{\text{min}}$ and $F(Z_R)_{\text{av}}$ is at best subject to considerable uncertainty. It has the defect that variable lengths of image trails on the photographic plates could not be taken into account. A vertically descending meteor or a meteor descending at a large angle to the zenith could not even approximately occupy its most favorable field position for dense exposure, as computed by the method of appendix C, except for a small fraction of its total path length. But a meteor descending with moderate obliquity could occupy nearly its most favorable field position throughout most of its path length.

Equation (45) appears to be the best revision of equation (40) that can be found at this time to conform with the data presented in reference 2. If possible, use of the function $F(Z_R)_{\text{av}}$ rather than $F(Z_R)_{\text{min}}$ is desirable for application to all meteors rather than to those of a selected group. The function $F(Z_R)_{\text{av}}$ was designed to provide the statistically expected value of E_{eff} according to equation (17) for any meteor selected at random. The function $F(Z_R)_{\text{min}}$, however, was provided only to apply specifically to the 100 test meteors and was provided only because no way was found to test $F(Z_R)_{\text{av}}$ directly. That is, no way was found to select a group of test meteors that should all have produced near marginal exposure density and which should have occurred in scattered locations throughout the field of view, rather than predominantly in the most favorable locations. However, it was believed that the defects in the manner of obtaining the functions as described earlier apply to the function $F(Z_R)_{\text{min}}$ more than to the function $F(Z_R)_{\text{av}}$. For that reason, little actual difference was believed to exist between use of one function or the other, as long as the correct exponents are used in equation (43) for each case, as will now be discussed.

Figure 8 is analogous to figure 7 as previously described, but applies to the function

$F(Z_R)_{av}$ rather than to the function $F(Z_R)_{min}$. In a manner similar to the earlier treatment of the function $F(Z_R)_{min}$, the function $F(Z_R)_{av}$ may be represented as

$$F(Z_R)_{av} = (\cos Z_R)^{-0.849} F'(Z_R)_{av} \quad (E5)$$

where $F'(Z_R)_{av}$ does not contain a power of $\cos Z_R$ as a factor.

If $F(Z_R)_{av}$ from equation (E5) is substituted for $F(Z_R)$ in equation (43), the following equation is obtained as a tentative substitute for equation (E3):

$$C_{marg} = m_{\infty}^{1.02} v_{\infty}^{\mu} (\cos Z_R)^{(\nu+0.849\xi)} F'(Z_R)_{av}^{\xi} \quad (E6)$$

No basis exists to distribute the exponent in the factor $(\cos Z_R)^{0.625}$ in equation (E3) between a corrected value of ν and a corrected value of the product -1.51ξ . Hence, apparently nothing better can be done with equation (E6) than to equate μ to 2.93, equate $(\nu + 0.849\xi)$ to 0.625, and equate ξ to -0.54. Accordingly, equation (E6) becomes

$$C_{marg} = m_{\infty}^{1.02} v_{\infty}^{2.93} (\cos Z_R)^{0.167} \left[(\cos Z_R)^{-0.849} F'(Z_R)_{av} \right]^{-0.54} \quad (E7)$$

Equation (E7) may be rewritten as equation (46).

If the value of C_{marg} of equation (46) or (E7) divided by the value of C_{marg} of equation (45) is regarded as a comparison factor φ_{comp} , then from equations (45), (E2), (E5), and (E7),

$$\varphi_{comp} = (\cos Z_R)^{0.356} \left[\frac{F(Z_R)_{min}}{F(Z_R)_{av}} \right]^{0.54} \quad (E8)$$

The curve in figure 9 shows the results of calculation of φ_{comp} according to equation (E8) with use of the mean values of $F(Z_R)_{min}$ and $F(Z_R)_{av}$ that are plotted in figures 7 and 8. As the absolute value of C_{marg} in equations (45) and (46) is of no interest, the absolute level of the comparison curve in figure 9 is also unimportant. If the statistically unimportant region between $\cos Z_R = 0.2$ and $\cos Z_R = 0.3$ is ignored, the comparison curve shows a range of logarithmic values of only about $\pm \log 1.08$. This variation amounts to only about ± 0.08 magnitude.

It is seen, therefore, that equation (46) or equation (E7) is very closely equivalent to equation (45). As at least a slight theoretical preference exists for use of $F(Z_R)_{av}$ instead of $F(Z_R)_{min}$, equation (46) will be used as a discovery criterion, in preference to equation (45).

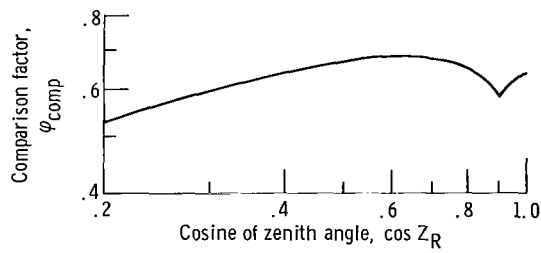


Figure 9. - Comparison factor involved in substitution of average for minimum statistical function of zenith angle.

APPENDIX F

EFFECT OF DIFFUSE EXPOSURE THRESHOLD ON DERIVATION OF BIAS CORRECTION FACTOR

Equation (60) was derived as a tentative expression for a bias correcting factor, to be modified later to account for the effect of altitude on area of the field of view of the cameras. The derivation of equation (60) was based on an assumption of a sharply defined level of exposure necessary for discovery of a meteor trail. It will be argued here that an assumption of a diffuse level of exposure necessary for discovery according to any postulated distribution law would not change the result.

In practice, in all probability, the sharply defined exposure level would not exist as a criterion for discovery of a meteor trail. Instead, observational failure would occur gradually throughout a range of exposures according to some unknown distribution. In figure 10, an illustration of an imaginary condition believed to be the statistical equivalent of the real condition is shown. The ordinate scale represents effective exposures in unspecified units. The position zero represents the highest level at which no meteors are ever discovered on the photographic plates. The abscissa scale, in unspecified units, represents simply a number of photographic plates arranged in an unspecified order.

Photographic plates arranged within an initial increment of abscissa are assumed to have been examined by the first of an indefinitely large number of observers who unfailingly detected all meteor trails down to the zero position on the scale of effective exposure. Observer 2 examined the plates arranged within a second increment of abscissa and unfailingly detected all meteor trails, but only down to an effective exposure level somewhat higher than that achieved by observer 1. Later observers examined the plates arranged within successively later increments of abscissa, and all observers detected trails unfailingly down to definite threshold levels. Those levels were higher with each successive observer, and in no case was any meteor detected below those levels.

At the right of figure 10 is shown an assumed curve governing success in discovery of trails for the real condition. The area to the right of this curve and below a given horizontal line represents the fraction of meteors discovered at the effective exposure level represented by that horizontal line.

Now, for example, at the exposure level of 3, one-half the meteors would be discovered according to the area to the right of the discovery curve and below that level; and, as illustrated, one-half the observers would discover all meteor trails down at least to that level of exposure. For any other exposure level, the area to the right of the

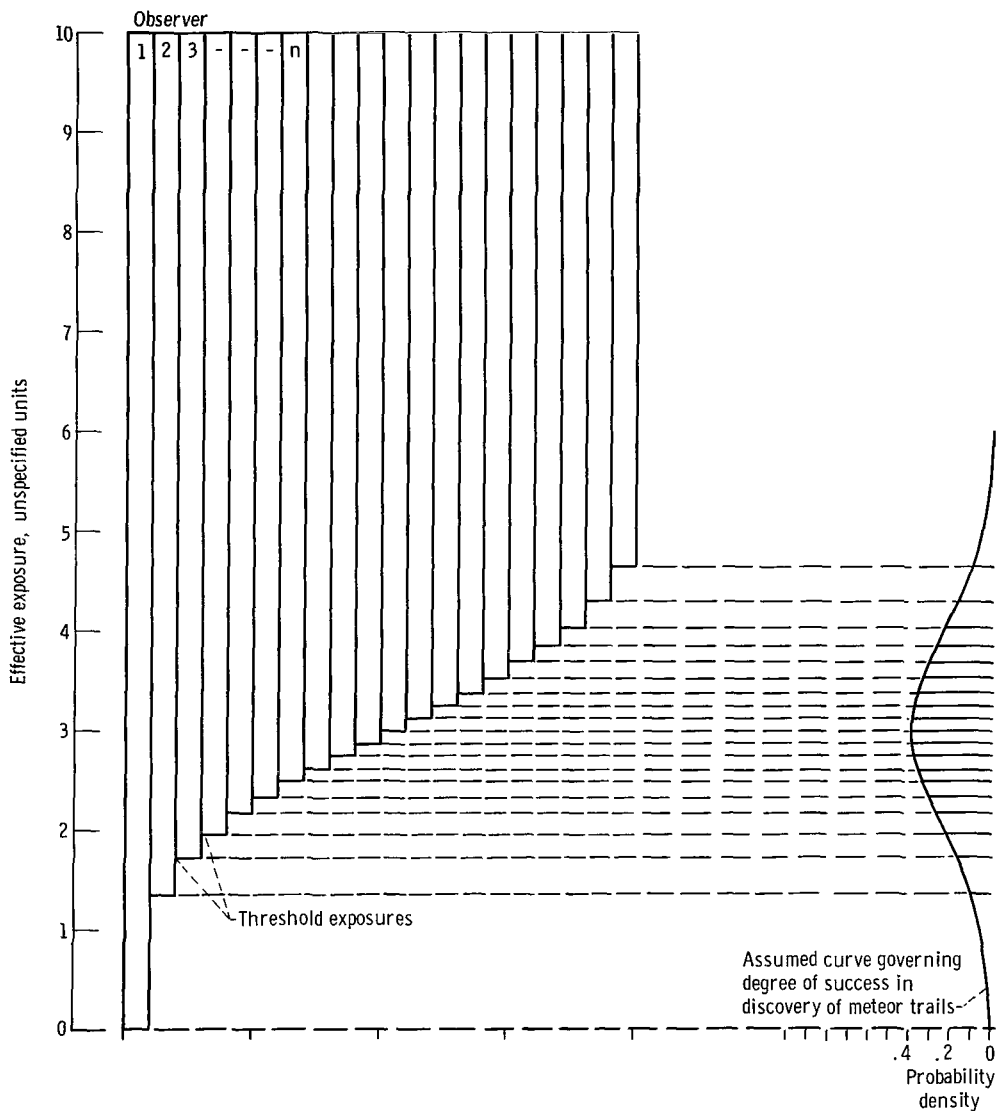


Figure 10. - Distribution of efforts of series of observers statistically equivalent to real condition in discovery of meteor trails.

discovery curve and below that exposure level is likewise proportional to the fraction of the observers who detect all meteors down at least to such exposure level.

Any observer n considered in figure 10 produces a series of observed values $F_{io(n)}$, $F_{jo(n)}$, $F_{ko(n)}$. Each observer, by use of the factor φ_w of equation (75), can deduce from his values $F_{io(n)}$, $F_{jo(n)}$, $F_{ko(n)}$ a correctly proportioned set of real values $F_{>m(i)}$, $F_{>m(j)}$, $F_{>m(k)}$, because his individual marginal exposure level does not appear in the correction factor. Hence, all observers collectively can obtain the correctly proportioned set of real values by the same method. That is, for any two subclasses such as i and j , equation (2) shows

$$\frac{F_{>m(i)}}{F_{>m(j)}} = \frac{\varphi_{w(i)} F_{io(n)}}{\varphi_{w(j)} F_{jo(n)}} \quad (F1)$$

and, as all values of $F_{io(n)}/F_{jo(n)}$ must therefore be the same,

$$\frac{F_{>m(i)}}{F_{>m(j)}} = \frac{\varphi_{w(i)} \sum_{n=1}^{\infty} F_{io(n)}}{\varphi_{w(j)} \sum_{n=1}^{\infty} F_{jo(n)}} \quad (F2)$$

It may be seen, however, that

$$F_{po} = \sum_{n=1}^{\infty} F_{po(n)} \quad (F3)$$

where p represents either i or j and F_{po} is the total count of meteors within velocity-zenith-angle class p by all observers. Hence, equation (2) may be written from equations (F2) and (F3), and it follows that the weighting factor $\varphi_{w(i)}$, $\varphi_{w(j)}$, and $\varphi_{w(k)}$ applied to the total counts F_{io} , F_{jo} , and F_{ko} according to equation (2) must yield the correct ratios of $F_{>m(i)}$, $F_{>m(j)}$, $F_{>m(k)}$, even for the condition of a diffuse exposure threshold.

A normal distribution curve was used for the discovery curve in figure 10. The same reasoning, however, would apply for any possible discovery curve that might apply to the real condition. Moreover, the statistical effect should be no different if, instead of the condition that was assumed, it were assumed (1) that a single observer examined all plates and (2), for whatever reason, at each moment during his operations

his effectiveness duplicated, at random, the effectiveness of one or another of the various observers that were postulated in the construction of figure 10.

REFERENCES

1. Whipple, Fred L.: Photographic Meteor Orbits and Their Distribution in Space. *Astronom. J.*, vol. 59, 1954, pp. 201-217.
2. McCrosky, Richard E.; and Posen, Annette: Orbital Elements of Photographic Meteors. *Smithsonian Contributions to Astrophysics*, vol. 4, no. 2, 1961, pp. 15-84.
3. Watson, Fletcher G.: *Between the Planets*. The Blakiston Co., Philadelphia, 1941.
4. Hawkins, Gerald S.; and Upton, Edward K. L.: The Influx Rate of Meteors in the Earth's Atmosphere. *Astrophys. J.* vol. 128, no. 3, Nov. 1958, pp. 727-735.
5. Whipple, Fred L.: Meteors and the Earth's Upper Atmosphere. *Rev. Mod. Phys.*, vol. 15, no. 4, Oct. 1943, pp. 246-264.
6. Öpik, Ernst J.: *Physics of Meteor Flight in the Atmosphere*. Interscience Publ., Inc., 1958.
7. Levin, B. Yu.: *The Physical Theory of Meteors, and Meteoric Matter in the Solar System, Chapters I-III*. American Meteorological Society, 1956. (Available from DDC as AD-110091.) (Translation from Akad. Nauk SSSR, Knigi Izdatel'stva.)
8. Jacchia, Luigi G.: *Photographic Meteor Phenomena and Theory. Meteor Photometry, Fundamental Equations and Constants, Durations and Flares*. Tech. Rep. No. 3, Harvard College Observatory, 1949.
9. Hawkins, Gerald S.; and Southworth, Richard B.: The Statistics of Meteors in the Earth's Atmosphere. *Smithsonian Contributions to Astrophysics*, vol. 2, no. 11, 1958, pp. 349-364.
10. Anon.: *U.S. Standard Atmosphere, 1962*. NASA, USAF, and U.S. Weather Bureau, Dec. 1962.
11. Öpik, Ernst: *Atomic Collisions and Radiation of Meteors*. Repr. No. 100, Harvard College Observatory, 1933.
12. Verniani, Franco: *On the Luminous Efficiency of Meteors*. Special Rep. No. 145 (NASA CR-55904), Smithsonian Astrophysical Observatory, Feb. 17, 1964.
13. Whipple, Fred L.; and Jacchia, Luigi G.: *Reduction Methods for Photographic Meteor Trails*. *Smithsonian Contributions to Astrophysics*, vol. 1, no. 2, 1957, pp. 183-206.
14. Jacchia, Luigi G.: *The Physical Theory of Meteors. VIII. Fragmentation as Cause of the Faint-Meteor Anomaly*. *Astrophys. J.*, vol. 121, no. 2, Mar. 1955, pp. 521-527.

15. Hawkins, Gerald S.: The Method of Reduction of Short-Trail Meteors. Smithsonian Contributions to Astrophysics, vol. 1, no. 2, 1957, pp. 207-214.
16. Whipple, Fred L.: The Harvard Photographic Meteor Program. Sky and Telescope, vol. 8, no. 4, Feb. 1949, pp. 90-93.
17. Lovell, Alfred C. B.: Meteor Astronomy. Clarendon Press, Oxford, 1954.
18. Jacchia, Luigi G.; and Whipple, Fred L.: The Harvard Photographic Meteor Programme. Vistas in Astronomy. Vol. 2, Arthur Beer, ed., Pergamon Press, 1956, pp. 982-994.

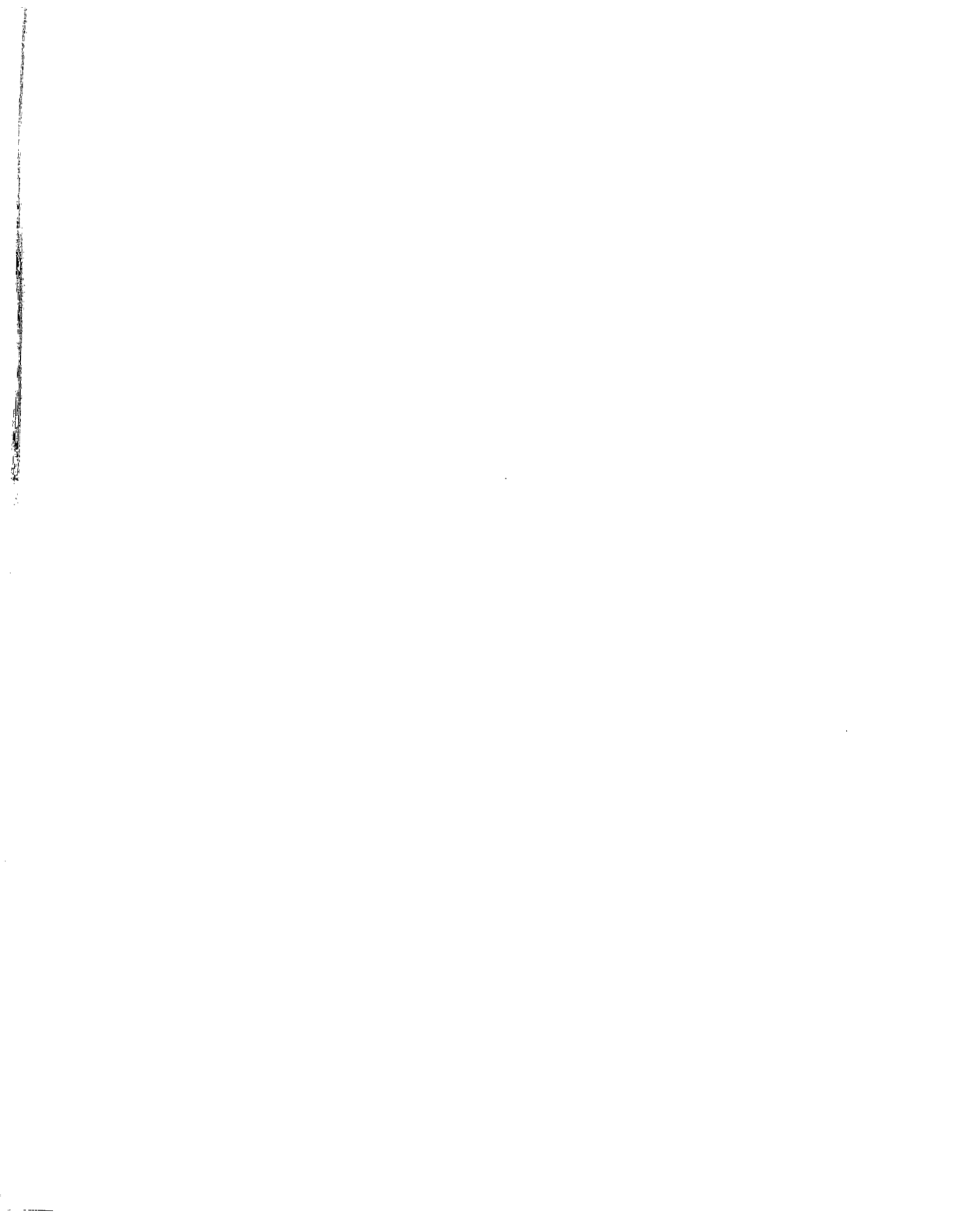


TABLE I. - 100 TEST METEORS PROVIDING

Subclass	Lower limit of meteoroid velocity in class, v_{co} , km/sec	Upper limit of meteoroid velocity in class, v_{co} , km/sec	Lower limit of cosine of zenith angle in subclass, $\cos Z_R$	Upper limit of cosine of zenith angle in subclass, $\cos Z_R$	Number of meteors in subclass	Serial number of meteor with maximum adjusted photographic magnitude, M_{adj}	Serial number of test meteor
1	0.0	15.5	0.20	0.48	25	4 008	9 057
2	↓	↓	.49	.64	24	12 175	5 087
3	↓	↓	.65	.72	24	4 372	11 884
4	↓	↓	.73	.80	24	7 203	12 353
5	↓	↓	.81	.85	24	6 135	5 058
6	↓	↓	.86	.89	27	12 651	8 312
7	↓	↓	.90	.91	22	4 114	11 797
8	↓	↓	.92	.94	30	6 076	6 268
9	↓	↓	.95	.97	20	7 735	4 905
10	↓	↓	.98	.99	21	10 196	7 170
11	15.5	17.5	0.20	0.53	18	12 715	5 050
12	↓	↓	.54	.65	17	7 461	4 964
13	↓	↓	.66	.73	19	11 964	12 150
14	↓	↓	.74	.81	17	4 842	4 722
15	↓	↓	.82	.86	18	7 745	6 300
16	↓	↓	.87	.88	15	7 252	12 513
17	↓	↓	.89	.92	18	10 295	5 948
18	↓	↓	.93	.95	18	6 985	11 892
19	↓	↓	.96	.97	17	7 226	7 755
20	↓	↓	.98	.99	17	7 293	7 244
21	17.5	20.5	0.20	0.49	21	6 350	9 252
22	↓	↓	.50	.63	23	7 719	7 721
23	↓	↓	.64	.68	20	10 223	7 924
24	↓	↓	.69	.77	24	7 207	12 515
25	↓	↓	.78	.82	21	3 344	7 324
26	↓	↓	.83	.87	30	4 795	7 375
27	↓	↓	.88	.89	14	7 303	10 208
28	↓	↓	.90	.93	22	6 981	8 363
29	↓	↓	.94	.97	22	8 771	7 504
30	↓	↓	.98	.99	19	6 875	12 233
31	20.5	23.5	0.20	0.56	21	6 363	10 480
32	↓	↓	.57	.66	17	7 070	10 542
33	↓	↓	.67	.74	17	10 027	9 398
34	↓	↓	.75	.80	18	8 189	6 889
35	↓	↓	.81	.82	18	4 148	4 575
36	↓	↓	.83	.86	18	6 286	12 171
37	↓	↓	.87	.90	20	6 387	7 965
38	↓	↓	.91	.93	16	4 203	8 790
39	↓	↓	.94	.97	19	4 967	7 643
40	↓	↓	.98	.99	17	7 506	11 805
41	23.5	27.5	0.20	0.52	21	7 802	3 079
42	↓	↓	.53	.66	23	7 622	8 202
43	↓	↓	.67	.72	21	4 505	11 809
44	↓	↓	.73	.79	24	8 413	12 478
45	↓	↓	.80	.82	21	6 992	7 228
46	↓	↓	.83	.87	25	7 118	4 582
47	↓	↓	.88	.90	19	10 498	10 168
48	↓	↓	.91	.93	23	5 003	12 452
49	↓	↓	.94	.96	19	5 351	4 977
50	↓	↓	.97	.99	21	6 069	6 254

APPROXIMATELY EQUAL EXPOSURE DENSITIES

Location of test meteor in ref. 2		Maximum adjusted photographic magnitude in subclass, M_{adj}	Photographic magnitude for test meteor, M_{pg}	Adjusted photographic magnitude for test meteor, M_{adj}	Initial mass as stated in reference 2 for test meteor, g	Cosine zenith angle of test meteor, $\cos Z_R$	Meteoroid velocity for test meteor, v_{∞} , km/sec	Minimum function of zenith angle, $F(Z_R)_{min}$	Weighted average function of zenith angle, $F(Z_R)_{av}$
Page	Line								
71	12	10.48	2.0	9.55	0.022	0.29	13.5	0.849	1.021
73	34	10.09	2.0	9.75	.035	.59	15.3	.580	.853
50	4	10.19	2.1	9.76	.076	.68	15.2	.525	.809
54	33	10.01	2.4	9.92	.031	.75	13.0	.388	.695
73	25	11.10	2.6	10.24	.027	.83	14.9	.274	.581
62	11	10.63	2.4	9.89	.030	.87	13.5	.235	.517
49	20	9.95	2.2	9.85	.040	.91	15.0	.179	.446
36	46	11.05	2.9	10.55	.043	.94	15.2	.175	.402
72	17	10.16	2.4	10.05	.022	.95	14.8	.168	.396
46	1	10.40	3.0	10.15	.120	.98	10.5	.159	.435
73	24	11.03	1.6	9.51	0.068	0.37	16.9	0.814	0.995
72	44	10.38	1.7	9.50	.130	.60	15.9	.605	.867
53	41	10.60	2.2	9.89	.049	.73	15.5	.407	.716
70	18	10.19	2.3	10.03	.019	.76	15.8	.405	.701
37	12	10.72	1.6	9.43	.016	.85	16.5	.229	.547
56	16	10.38	2.5	10.33	.021	.88	17.4	.225	.519
82	40	9.95	1.5	9.31	.058	.90	17.3	.175	.462
50	8	10.30	2.3	10.10	.0083	.93	16.0	.164	.414
56	6	9.90	2.0	9.89	.0082	.96	17.3	.173	.392
46	31	9.91	1.9	9.85	.012	.99	17.1	.173	.382
76	11	9.95	1.7	9.68	0.050	0.45	19.8	0.741	0.955
55	28	10.47	2.5	10.39	.013	.63	17.6	.591	.861
57	42	10.10	1.7	9.79	.031	.67	20.1	.483	.777
56	17	10.97	2.7	10.67	.022	.71	19.1	.499	.785
47	15	10.33	1.9	9.92	.014	.82	19.4	.304	.606
47	37	10.42	2.3	10.38	.012	.84	20.0	.248	.562
40	27	10.17	1.8	9.87	.029	.88	20.4	.213	.509
62	29	11.35	3.2	11.13	.016	.93	17.6	.181	.414
50	49	10.41	2.1	9.97	.020	.95	17.9	.154	.383
37	48	10.15	2.0	10.03	.0099	.98	20.2	.175	.377
44	49	10.31	1.9	10.20	0.057	.25	22.7	0.878	1.029
46	10	10.65	2.1	10.26	.0068	.66	21.2	.492	.791
78	1	10.33	2.1	10.28	.032	.74	22.0	.444	.737
41	46	10.32	1.9	9.90	.011	.78	23.3	.370	.668
68	19	10.10	1.8	10.03	.021	.81	22.5	.353	.656
53	47	10.34	1.8	9.95	.0069	.84	22.3	.304	.605
59	22	10.52	2.3	10.27	.0097	.87	21.7	.224	.505
69	23	10.74	2.4	10.65	.012	.91	23.4	.181	.439
52	22	10.63	1.8	9.91	.026	.97	20.9	.161	.376
49	23	10.84	2.2	10.38	.012	.98	22.6	.169	.385
43	25	10.61	2.0	10.33	0.0093	0.42	25.7	0.759	0.967
61	39	10.76	1.6	9.88	.028	.56	25.1	.617	.879
49	25	10.26	1.8	10.24	.0060	.72	27.3	.404	.722
55	41	9.99	1.6	9.99	.011	.73	25.3	.415	.717
46	27	10.36	1.9	10.17	.010	.81	23.7	.344	.648
68	21	11.35	2.0	10.50	.0047	.87	26.4	.242	.542
40	9	11.27	2.7	10.96	.0035	.89	24.4	.173	.469
55	25	10.31	1.8	10.16	.0082	.91	25.4	.154	.431
72	49	10.73	2.1	10.41	.010	.96	24.9	.175	.388
36	39	11.81	1.9	10.27	.012	.98	26.9	.170	.382

TABLE I. - Concluded. 100 TEST METEORS PROVIDING

Subclass	Lower limit of meteoroid velocity in class, v_{∞} , km/sec	Upper limit of meteoroid velocity in class, v_{∞} , km/sec	Lower limit of cosine of zenith angle in subclass, $\cos Z_R$	Upper limit of cosine of zenith angle in subclass, $\cos Z_R$	Number of meteors in subclass	Serial number of meteor with maximum adjusted photographic magnitude, M_{adj}	Serial number of test meteor
51	↓	↓	0.20	0.57	18	9 037	9 406
52			.58	.64	20	8 777	8 106
53			.65	.71	19	7 116	8 767
54			.72	.78	24	6 847	7 145
55			.79	.81	13	6 887	5 380
56			.82	.85	20	8 028	4 507
57			.86	.88	19	8 849	12 570
58			.89	.91	18	12 548	4 556
59			.92	.97	24	12 318	9 025
60			.98	.99	14	9 182	3 028
61	↓	↓	0.20	0.49	20	7 073	6 424
62			.50	.62	22	12 672	12 180
63			.63	.68	19	5 439	7 813
64			.69	.74	26	6 496	7 114
65			.75	.80	15	4 744	7 108
66			.81	.83	20	10 321	7 433
67			.84	.88	27	4 510	4 418
68			.89	.92	16	7 395	11 783
69			.93	.96	20	5 298	4 406
70			.97	.99	20	5 419	9 007
71	↓	↓	0.20	0.52	20	4 933	7 339
72			.53	.60	20	6 114	3 419
73			.61	.67	20	6 964	5 027
74			.68	.75	23	6 403	8 530
75			.76	.79	15	8 065	8 788
76			.80	.84	21	8 522	8 030
77			.85	.88	22	4 434	4 750
78			.89	.92	18	12 068	8 257
79			.93	.96	21	4 094	6 537
80			.97	.99	18	6 206	7 414
81	↓	↓	0.20	0.42	20	6 471	5 437
82			.43	.53	19	6 516	4 552
83			.54	.59	20	7 771	7 545
84			.60	.67	21	7 874	4 781
85			.68	.73	21	5 294	5 204
86			.74	.80	18	12 108	6 636
87			.81	.87	22	4 567	4 609
88			.88	.92	19	4 694	11 178
89			.93	.96	20	9 046	12 763
90			.97	.99	20	5 034	3 204
91	↓	∞	0.20	0.41	20	4 424	6 071
92			.42	.50	19	6 320	8 245
93			.51	.57	22	4 416	6 952
94			.58	.63	18	6 521	8 477
95			.64	.69	21	4 668	5 491
96			.70	.75	21	5 284	8 892
97			.76	.81	19	6 518	8 350
98			.82	.86	21	6 150	8 520
99			.87	.93	19	4 410	4 650
100			.94	.99	20	4 408	6 011

APPROXIMATELY EQUAL EXPOSURE DENSITIES

Location of test meteor in ref. 2		Maximum adjusted photographic magnitude in subclass, M_{adj}	Photographic magnitude for test meteor, M_{pg}	Adjusted photographic magnitude for test meteor, M_{adj}	Initial mass as stated in reference 2 for test meteor, g	Cosine zenith angle of test meteor, $\cos Z_R$	Meteoroid velocity for test meteor, v_{∞} , km/sec	Minimum function of zenith angle, $F(Z_R)_{min}$	Weighted average function of zenith angle, $F(Z_R)_{av}$
Page	Line								
78	4	10.26	1.7	10.12	0.027	0.52	27.5	0.651	0.905
60	9	10.02	1.5	10.00	.020	.64	29.9	.553	.824
69	11	10.39	1.8	10.37	.0099	.66	31.1	.549	.825
45	39	10.43	1.5	9.97	.0062	.78	28.4	.379	.680
76	35	10.76	2.1	10.67	.0046	.81	31.1	.306	.610
67	39	10.81	2.0	10.49	.0088	.82	29.0	.293	.596
57	5	11.77	2.3	10.71	.0032	.88	28.0	.224	.521
68	12	10.54	2.0	10.50	.0056	.91	29.8	.197	.444
70	49	10.46	2.0	10.45	.0069	.95	27.7	.170	.392
43	39	10.97	1.9	10.57	.0032	.98	30.2	.176	.383
39	6	10.38	1.6	10.24	0.0041	0.39	32.5	0.770	0.979
37	35	10.88	1.6	10.36	.0031	.52	36.0	.649	.904
56	35	10.45	1.5	10.27	.0051	.65	33.8	.508	.799
45	30	10.99	1.9	10.53	.0042	.74	31.8	.417	.714
45	19	10.85	1.8	10.48	.0045	.78	32.2	.319	.645
48	8	11.10	2.0	10.77	.0028	.83	33.4	.257	.575
67	2	10.62	1.7	10.42	.0048	.88	35.0	.197	.488
49	13	10.29	1.4	10.16	.0018	.89	37.0	.172	.470
66	46	10.81	2.0	10.81	.0011	.94	37.1	.176	.407
70	43	10.69	1.8	10.40	.0065	.99	31.9	.161	.376
47	22	10.54	1.2	10.34	0.0046	0.37	44.6	0.813	0.995
60	37	10.53	1.4	10.26	.0045	.56	40.4	.662	.909
73	15	10.71	1.6	10.67	.0014	.66	48.4	.546	.822
63	45	10.67	1.5	10.45	.0015	.73	43.2	.420	.718
69	22	10.37	1.1	10.26	.0021	.79	47.6	.324	.633
59	35	10.74	1.5	10.43	.0011	.81	40.8	.348	.652
71	10	10.58	1.5	10.52	.0015	.87	45.3	.204	.506
62	5	10.70	1.6	10.65	.00092	.92	47.8	.164	.423
39	46	10.40	1.4	10.35	.0016	.93	42.5	.170	.413
48	3	10.70	1.5	10.48	.0015	.98	41.9	.160	.383
77	16	10.35	1.0	10.31	0.0012	0.21	55.7	0.898	1.043
68	10	10.65	1.1	10.53	.0013	.50	54.2	.717	.945
51	23	10.61	1.0	10.43	.0013	.54	61.6	.643	.894
71	23	11.62	1.3	10.75	.00048	.67	59.2	.468	.776
74	23	11.44	1.1	10.53	.001	.73	61.6	.458	.752
84	9	10.40	1.0	10.37	.00079	.80	62.5	.308	.620
68	29	10.77	1.2	10.74	.00075	.85	63.4	.276	.573
48	40	11.07	1.7	10.93	.00071	.89	63.3	.189	.470
38	27	10.90	1.4	10.80	.00056	.95	56.5	.176	.396
47	33	11.26	1.5	10.45	.00067	.97	52.5	.170	.378
35	13	10.52	0.9	10.50	0.00034	0.23	63.7	0.887	1.037
62	1	10.62	.9	10.51	0.00057	0.49	63.8	0.675	0.924
42	17	10.68	.9	10.46	.00052	.56	65.5	.654	.901
63	20	10.84	1.0	10.66	.00045	.58	68.2	.584	.859
77	36	10.64	.9	10.53	.00059	.68	69.7	.525	.809
70	8	11.02	1.4	10.94	.00073	.70	67.1	.449	.745
62	28	11.07	1.2	10.81	.00049	.81	68.7	.277	.601
63	40	10.89	1.2	10.80	.00033	.86	68.9	.228	.522
68	42	11.59	1.2	10.74	.00076	.88	68.9	.212	.509
83	34	11.78	1.4	10.93	.00030	.98	65.6	.175	.380

"The aeronautical and space activities of the United States shall be conducted so as to contribute . . . to the expansion of human knowledge of phenomena in the atmosphere and space. The Administration shall provide for the widest practicable and appropriate dissemination of information concerning its activities and the results thereof."

—NATIONAL AERONAUTICS AND SPACE ACT OF 1958

NASA SCIENTIFIC AND TECHNICAL PUBLICATIONS

TECHNICAL REPORTS: Scientific and technical information considered important, complete, and a lasting contribution to existing knowledge.

TECHNICAL NOTES: Information less broad in scope but nevertheless of importance as a contribution to existing knowledge.

TECHNICAL MEMORANDUMS: Information receiving limited distribution because of preliminary data, security classification, or other reasons.

CONTRACTOR REPORTS: Scientific and technical information generated under a NASA contract or grant and considered an important contribution to existing knowledge.

TECHNICAL TRANSLATIONS: Information published in a foreign language considered to merit NASA distribution in English.

SPECIAL PUBLICATIONS: Information derived from or of value to NASA activities. Publications include conference proceedings, monographs, data compilations, handbooks, sourcebooks, and special bibliographies.

TECHNOLOGY UTILIZATION PUBLICATIONS: Information on technology used by NASA that may be of particular interest in commercial and other non-aerospace applications. Publications include Tech Briefs, Technology Utilization Reports and Notes, and Technology Surveys.

Details on the availability of these publications may be obtained from:

SCIENTIFIC AND TECHNICAL INFORMATION DIVISION
NATIONAL AERONAUTICS AND SPACE ADMINISTRATION
Washington, D.C. 20546